Nitrogen Excretion in the Freshwater Dwelling Ribbon Leech (*Nephelopsis obscura*)

by

Alex R. Quijada-Rodriguez

A Thesis submitted to the Faculty of Graduate Studies of
The University of Manitoba
in partial fulfillment of the requirements of the degree of

MASTER OF SCIENCE

Department of Biological Sciences
University of Manitoba
Winnipeg

Abstract

Remarkably little is known about nitrogenous excretion in freshwater invertebrates. In the current study, the nitrogen excretion mechanism in the carnivorous ribbon leech, *Nephelopsis obscura,* was investigated. Based on gene expression analysis and Ussing chamber experiments, the skin was identified as a major site of ammonia excretion. Pharmacological experiments and enzyme assays suggested an ammonia excretion mechanism that involves the V-ATPase, Na^+/K^+-ATPase and carbonic anhydrase, but not necessarily a functional microtubule system. Most importantly, functional expression studies of the identified Rh-protein cloned from leech skin (NoRhp) revealed an ammonia transport capability of this protein when expressed in yeast. Exposure to high environmental ammonia (HEA) caused a new adjustment of body ammonia, accompanied with a decrease in NoRhp and Na^+/K^+-ATPase mRNA levels, but unaltered ammonia excretion rates. The results of this study showed many similarities to the ammonia excretion mechanisms proposed in the gills of freshwater fish.

Acknowledgements

First and foremost I would like to thank my advisor, Dr. Dirk Weihrauch, for his support encouragement, extreme patience and most importantly belief in my abilities as a graduate student throughout my thesis project. Throughout my time knowing Dirk he has always worked hard to develop his students into researchers which aim to maintain a high quality of scientific research and he has always provided us all the opportunities available to collaborate and network with various top researcher in our field for this I am very grateful. There is no lab I would have rather spent these last two years in as his enthusiasm and passion for this wonderful field of ion transport physiology has surely done wonders in my development as a researcher. I would also like to thank my committee members Dr. Jason Treberg and Dr. Georg Hausner for their constructive criticism and guidance along the way. I would also like to express my deepest gratitude to my collaborators Drs. Greg Goss, Aaron Schultz, David Boyle, Anna Maria Marini, and Mélanie Boeckstaens without them this thesis would not be possible.

To my fellow members of the crab lab Stephanie Hans, Sandra Fehsenfeld, Aida Adlimoghaddam, and Joana Correia thank you for always being there to provide technical and moral support through both the highs and lows of my thesis work. There are also a number of professors in the department who have provided lab space, equipment, technical advice and sometimes just a good laugh who I would like thank these include: Drs. Kevin Campbell, Gary Anderson, Mark Fry, Steve Whyard, and Michelle Piercy-Normore. I would also like to thank the various friends and colleagues that have made my M.Sc. extremely enjoyable while also providing help along the way these include: Kelsey O'Brien, Anthony Signore, Michael Gaudry, Cameron Bauer, Samantha Lee, Cassidy Erdelyan, Cole Robson-Hyska, Alex Hare, Ben Kissinger, Duncan Burnett, Calen Ryan, Michelle Ewacha, Jen Sojka, Darcy Childs, Michael

Becker, Catherine Brandt, Dr. Kai He, Kyle Fontaine, and Chris Deduke. Lastly, I would like to thank my parent Jose Antonio Quijada-Sanchez and Nora Rodriguez as well as my siblings Francisco Rodriguez, Mario Quijada-Rodriguez, Angela McEvoy, brother in law Caolan McEvoy and nephew Rory McEvoy who have always supported me throughout my academic journey.

Thesis Contributions

A condensed form of this thesis excluding some data sets is currently in revision by the American Journal of Physiology: Regulatory, Integrative and Comparative Physiology (submission date: December 1, 2014; submission #: R-00482-2014). Data collected on the effects of ouabain, colchicine, acetazolamide, and concanamycin C as well as data collected on the effects of short-term environmental pH on ammonia excretion were performed, analyzed, and included in my Honours thesis (April 2012). In addition to this work from my Honours thesis, Dr. Jason Treberg performed and analyzed data pertaining to Na^+/K^+-ATPase enzyme assays. Aside from the aforementioned data sets, all other data in this thesis were collected and analyzed by Alex R. Quijada-Rodriguez.

Table of Content

List of Tables

List of Figures

1. Introduction

1.1 Ammonia toxicity

The majority of ammonia (in this study, NH_3 refers to non-ionic ammonia, NH_4^+ to ionic ammonia, and ammonia to the sum of both) in an organism is synthesized through the metabolic process of deamination, while uricolytic or ureolytic pathways usually account for a small portion of ammonia produced (Dimski, 1994; Meijer et al., 1990). In solution, ammonia (pKa=9.2 to 9.8) will be present in a pH-dependent equilibrium of the non-ionic, membrane-permeable form, NH_3, and the ionic form, NH_4^+ (Cameron and Heisler, 1983). As the pKa of ammonia is relatively high, the vast majority of ammonia present in the environment or body fluids will typically be in the ionic NH_4^+ form, unless fairly alkaline environments or body fluid conditions are present.

While inherently produced by all cells through protein metabolism, ammonia is highly toxic, exhibiting various detrimental effects. For example, ammonia is capable of affecting energy metabolism (Cooper and Plum, 1987; O'Donnell, 1997; Wilkie, 1997) and ion transport capabilities in vertebrates as well as invertebrates (Binstock and Lecar, 1969; Harris et al., 2001; Nakhoul et al., 2001). More specifically, one mode of toxicity includes the uncoupling of proton gradients across the inner mitochondrial membrane due to the binding of NH_3 to free H^+, resulting in a disruption of oxidative phosphorylation (O'Donnell, 1997). Furthermore, as extensively studied in mammals, ammonia has various detrimental effects on the central nervous system, such as cerebral edema, cerebral atrophy, and disturbances of neuronal growth and signal transduction pathways (Braissant et al., 2013). Some modes of toxicity in the central nervous system of mammals include prolonged N-methyl-D-aspartate (NMDA) receptor activation

and/or inhibition of GLAST and GLT-1 transporters preventing glutamate removal from neuronal synapses, both of which result in uncontrolled Ca^{2+} uptake and ATP depletion, eventually leading to cell death by excitotoxicity (Albrecht et al., 2010; Chan et al., 2000; Knecht et al., 1997; Marcaida et al., 1992; Norenberg et al., 1997). In addition to this, another mode of toxicity includes the increased conversion of glutamate to glutamine, an osmolyte, by glutamine synthetase, leading to astrocyte swelling and eventually cell death (Zwingmann and Butterworth, 2005).

1.2 Ammonia excretion mechanisms

Due to the high toxicity of ammonia, all animals must have an efficient mechanism by which ammonia is detoxified into less toxic nitrogenous waste products or rapidly excreted in order to maintain body fluid levels within a tolerable range. Typically, non-mammalian aquatic organisms excrete the majority of their nitrogenous waste as ammonia (Larsen et al., 2014; Wright, 1995).

Various studies have shown that ammonia transport occurs often via tissues also responsible for gas exchange and/or osmoregulation, such as skin (Cruz et al., 2013; Shih et al., 2008; Weihrauch et al., 2012b), intestine (Rubino et al., 2014; Weihrauch, 2006; Wilson et al., 2013), nephridial systems (Kulkarni et al., 1989; Lutz and Siddiq, 1971), gills (Weihrauch et al., 2009; Wright and Wood, 2009), kidneys (Wall and Koger, 1994), and anal papillae (Donini and O'Donnell, 2005; Weihrauch et al., 2012a). Early work on ammonia excretion suggested that transport of NH_3 was purely passive due to its permeability in lipid bilayers (Kormanik and Cameron, 1981) and the lack of identification of an NH_3 transporting protein. The discovery that

Rhesus glycoproteins (Rh proteins) in humans function as ammonia transporters (Marini et al., 2000) and the subsequent identification of Rh proteins expressed in ionoregulatory tissues of aquatic organisms (Weihrauch et al., 2004) have prompted further studies into the mechanism of ammonia transport in a variety of aquatic organisms. Mechanistic studies of ammonia excretion in aquatic organisms have mainly been focused on teleost fish, with a few studies conducted on marine decapod crabs (Weihrauch et al., 2004; Weihrauch et al., 2009; Wright and Wood, 2009). It is important to note that freshwater invertebrates from at least seven different phyla comprise approximately 85% of all described freshwater animal species (Balian et al., 2008) and to date, only a single comprehensive mechanistic study has been conducted on a freshwater invertebrate, the planarian *Schmidtea mediterranea* (Weihrauch et al., 2012b). With freshwater invertebrates remaining a highly understudied but highly diverse group of organisms, further investigations are critical to gain an understanding of the evolution of ammonia excretion mechanisms and to determine if there are general ammonia excretion strategies functioning in freshwater environments.

Thus far, mechanistic studies on the freshwater planarian *Schmidtea mediterranea* and freshwater fish have demonstrated ammonia excretion mechanisms dependent on acidification of an unstirred boundary layer on the apical side of the ammonia-transporting epithelia (Weihrauch et al., 2012b; Wilson et al., 1994; Wright and Wood, 2009). On the basolateral membrane, Na^+/K^+-ATPase transports blood ammonia into the cytoplasm of the epithelial cell where NH_4^+ is transported in place of K^+. In addition to this, basolateral Rh protein isoforms may potentially play a role in blood ammonia transport. In the cytoplasm, carbonic anhydrase (CA) catalyzes the hydration of carbon dioxide, forming H^+ that are then excreted into the apical unstirred boundary layer by V-ATPase and Na^+/H^+-exchanger. Furthermore, it has been proposed that membrane-

bound CA may hydrate CO_2 in the unstirred boundary layer, generating protons for the acidification of the unstirred boundary layer (Lin and Randall, 1991). This acidification causes a decrease in the partial pressure of NH_3 (P_{NH3}), which drives cellular excretion of NH_3 into the unstirred boundary layer via Rh proteins. In the unstirred boundary layer, NH_3 will combine with free H^+ to form ionic ammonia, which is incapable of diffusing back into the epithelia.

1.3 Leeches

The present study focuses on the freshwater ribbon leech *Nephelopsis obscura* (also called *Erpobdella obscura*) commonly found distributed throughout various freshwater bodies in Canada and northern USA (Davies, 1973). Unlike the more widely known blood feeding leeches, this species is carnivorous, feeding on a protein-rich diet comprised mainly of chironomids and small oligochaetes (Davies et al., 1978). While little is known about the nitrogen physiology of *N. obscura*, a number of studies have investigated sodium transport across the skin in other freshwater leeches (Clauss, 2001). From studies on the blood feeding medicinal leech *Hirudo medicinalis*, the skin has been identified as a site of sodium uptake (Weber et al., 1993; Weber et al., 1995), which may also potentially serve as the site of ammonia excretion due to the similarity in transporters (Na^+/K^+-ATPase, V-ATPase, and Na^+/H^+-exchanger) typically utilized for both processes (Larsen et al., 2014; Marshall, 2002; Parks et al., 2008). In addition to skin, other potential sites of ammonia transport include the metanephridia, where urine formation and $Na^+/Cl^-/K^+$ balance occur, as well as the intestine where food breakdown and amino acid uptake would occur (Clauss, 2001).

1.4 Aims and Objectives

The aim of this thesis was to build on my Honours thesis work and determine the mechanism of ammonia excretion in the skin of the freshwater ribbon leech *Nephelopsis obscura*. This was accomplished through whole animal excretion experiments, transport studies employing the isolated leech skin in Ussing chambers, gene expression analysis, and yeast complementation assays. In addition to examining the mechanism of ammonia excretion, the ability for *N. obscura* to regulate and adapt to internal ammonia loads was examined utilizing feeding and high environmental ammonia exposure experiments. The objectives of this study included:

1. Demonstrating that the leech skin is a major site of ammonia excretion by utilizing gene expression analysis of key transporters in the skin versus whole body, as well as skin mounted in Ussing chambers.

2. Determine the role of Na^+/K^+-ATPase and Na^+/H^+-exchangers in ammonia excretion by utilizing pharmacological agents in whole animal excretion experiments and/or isolated tissue in Ussing chambers.

3. Identify and functionally characterize a primitive Rhesus protein in the skin of *N. obscura* as an ammonia transporter.

4. Determine the effects of feeding on ammonia excretion on a whole animal basis as well as changes in gene expression in response to feeding.

5. Determine the effect of short and long-term high environmental ammonia (HEA) exposure on body ammonia, ammonia excretion, and gene expression of identified key transporters.

1.5 Hypotheses

1. The majority of ammonia excreted will occur over the skin, which will exhibit a higher mRNA expression level of key transporters involved in ammonia transport relative to the rest of the body.

2. Pharmacological inhibition of the Na^+/K^+-ATPase and Na^+/H^+-exchanger will cause reductions in ammonia excretion as these transporters are typically coupled or co-localized with other ammonia-transporting proteins.

3. Rhesus proteins in the skin of *N. obscura* will be capable of transporting ammonia when expressed in yeast as they contain key amino acids responsible for conducting ammonia transport.

4. Feeding will result in elevated ammonia excretion and mRNA expression of key transporters in order to compensate for internal ammonia load generated by amino acid metabolism.

5. Short-term (one hour) HEA will result in ammonia uptake while long-term (one and seven day) HEA will result in recovery of control ammonia excretion rates, elevated body ammonia, and elevated mRNA expression in order to compensate for environmental ammonia changes.

2. Methods

2.1 Animals

Leeches *(Nephelopsis obscura)* obtained from a local bait shop (Manny's Live Bait, Winnipeg, MB) were maintained at 10°C under natural lighting conditions (12h light: 12h dark) in 100 litres of dechlorinated tap water (DTW; pH ~8.3) and constantly aerated via air stones. Tank ammonia concentrations were maintained below 10 μmol l^{-1}. Leeches were fed frozen bloodworms twice a week for two hours *ad libitum*. Aquarium water was replaced six hours after each feeding period. All experiments were performed at 10°C on leeches starved for a minimum of two days.

2.2 Whole animal ammonia excretion experiments

For whole animal excretion experiments, individual leeches (ca. 0.5-3.7 grams of fresh weight (gFW), 2.54-12.7 cm in length) were placed into 100 ml beakers containing 30 ml of DTW (pH ~8.3), aerated by means of air stones. After a one-hour equilibration period, the media was replaced with a fresh volume of DTW for the initial sampling period. At the end of each sampling period, a 10 ml sample was taken and frozen (-20 °C) for later analysis of ammonia and urea. After each sampling period, the fluid in the beakers was discharged and animals subsequently rinsed with 50 ml of DTW.

2.2.1 Excretion experiments under the influence of various inhibitors and pH regimes

To determine ammonia excretion rates in media buffered to various pH regimes, a control sampling period (one hour DTW, pH 8.3) was followed by a one-hour sampling period in DTW buffered to a certain pH by either 5 mmol l^{-1} 2-(*N*-morpholino)ethanesulfonic acid (MES) (pH 5), or 5 mmol l^{-1} tris(hydroxymethyl) aminomethane hydrochloride (Tris-HCl) (pH 8.3 and 9.5). The pH of the experimental media was adjusted with HCl or NaOH.

In another set of experiments, the effect of pharmacological agents on ammonia excretion rates was investigated. Here, a rinse and a 30-minute pre-incubation period in a specific inhibitor (30 ml) followed the initial control-sampling period (one hour). A 5 ml sample was taken after the pre-incubation period and a one-hour experimental sampling period in the remaining media (25 ml) followed. Acetazolamide, concanamycin C, and 5-(N-ethyl-N-isopropyl)amiloride (EIPA) were dissolved in dimethyl sulfoxide (DMSO) at a final concentration of 0.5% in the experimental solution. DMSO was also added to the respective control experimental solutions for experiments involving these inhibitors. Inhibitors utilized in this study were applied at concentrations shown to be effective in other invertebrates (Weihrauch, 2006; Weihrauch et al., 1998; Weihrauch et al., 2002; Weihrauch et al., 2012b). The inhibitors utilized in this study were (in mmol l^{-1}): 5 sodium azide, 0.005 concanamycin C, 1 acetazolamide, 0.1 5-(N-Ethyl-N-isopropyl) amiloride (EIPA), 5 ouabain, and 2 colchicine. Following inhibitor experiments, no mortalities due to inhibitor treatments were observed in leeches monitored for one week.

2.2.2 Feeding experiments

When feeding experiments were performed, leeches were starved for five days and a feeding period (frozen bloodworms, *ad libitum*) of one hour in 80 ml of DTW followed the control measurement. After the feeding period, beakers were rinsed with DTW and 30 ml of fresh DTW was added for the first one-hour sampling period after feeding. As performed for the first sampling period, five consecutive one-hour sampling periods post feeding followed. After the sixth one-hour sampling period post-feeding, the integument of the leeches was dissected (see tissue preparation). If bloodworms were observed to be present in the leech intestine during the skin dissection (6h after feeding), samples were used for ammonia analysis. In parallel, another set of post-feeding leeches were maintained in 500 ml of DTW for 24 hours. After 24 hours post-feeding, leeches were transferred to 30ml DTW for a 24-hour after feeding sampling period.

2.2.3 High environmental ammonia experiments (HEA)

For HEA experiments, a control-sampling period (one hour ammonia free DTW, pH 8.3) was followed by two consecutive one-hour sampling periods. The first sampling period occurred in DTW enriched with 1 mmol l^{-1} NH_4Cl, while the second sampling period was in ammonia-free DTW. Following this, leeches were placed in a three-litre container of DTW enriched with 1 mmol l^{-1} NH_4Cl for one day. After a one-day HEA exposure, leeches underwent three consecutive one-hour sampling periods. The first and last sampling periods were done in DTW containing 1 mmol l^{-1} NH_4Cl and the second sampling period was done in ammonia-free DTW. Following these sampling periods, leeches were returned to the three-litre container with

1 mmol l^{-1} NH_4Cl for six more days. After seven days of HEA exposure, three consecutive one-hour sampling periods identical to that of one-day HEA acclimated leeches were performed. Leeches remained unfed during the course of this experiment to prevent additional internal ammonia buildup due to feeding.

2.3 Ussing chamber experiments

Leech skin was isolated (see tissue preparation) and mounted with Vetbond tissue adhesive (3M, St.Paul, MN, USA) in a modified Ussing chamber (P2300, Physiologic Instruments, San Diego, CA) with a 0.45 cm^2 aperture tissue holder. Experiments were performed at 10°C with experimental solutions maintained constantly aerated. Leech skin was bathed with unbuffered DTW (pH 8.3) containing 10 mmol l^{-1} theophylline on the apical side and leech Ringer's solution on the basolateral side. The leech Ringer's solution (pH 7.4) contained (in mmol l^{-1}): 115 NaCl, 1.8 $CaCl_2$, 2 $MgCl_2$, 4 KCl, and 10 HEPES (Tian et al., 2007). The leech Ringer's solution was further supplemented with 10 mmol l^{-1} glucose to provide an energy substrate for the tissue and 10 mmol l^{-1} theophylline, which has been shown to activate ammonia excretion in skin epithelia mounted in an Ussing chamber (Cruz et al., 2013). Chambers were filled with 4 ml of the corresponding experimental solutions stated above. Prior to all Ussing chamber experiments, a one-hour period in the corresponding experimental solutions indicated was given to allow for tissue equilibration. Unless otherwise mentioned, the experimental solutions during the incubation, washout, and equilibration periods were replaced with fresh solutions between each period.

For determination of metabolic ammonia released towards the apical side of the leech skin, a one-hour equilibration period was followed by three consecutive 1.5-hour sampling periods with no ammonia on either the basolateral or apical side. Following each sampling period, 4 ml samples were taken from both sides of the tissue and immediately frozen (-20°C) for later ammonia analysis, and fresh experimental solutions were added to the chambers.

For pharmacological studies examining the effects of ouabain, an inhibitor of Na^+/K^+-ATPase, on ammonia excretion, the leech Ringer's solution was further enriched with 300 μmol l^{-1} NH_4Cl, while the apical DTW contained no ammonia to provide an *in vivo*–like ammonia gradient across the tissue. Pharmacological Ussing chamber experiments consisted of six experimental time points: (1) one hour equilibration period, (2) one hour control sampling period, (3) 30 minute inhibitor incubation period (Ringer's enriched with 5 mmol l^{-1} ouabain), (4) one hour inhibitor sampling period (Ringer's enriched with 5 mmol l^{-1} ouabain), (5) 30 minute inhibitor washout period to remove excess ouabain from experimental chambers and tissue, and (6) one hour tissue integrity sampling period to verify that the tissue was still active by re-establishing control excretion levels. The measured apically-directed metabolic ammonia release by the tissue was subtracted from flux rates in pharmacological experiments to obtain values for ammonia excretion due to the active transport of basal ammonia.

2.4 Long-term HEA acclimation

Groups of leeches (six leeches in three litres) were maintained in 1 mmol l^{-1} NH_4Cl for one or seven days with experimental solutions changed daily. After the one or seven-day exposure time, leeches were cut in half and the posterior half of the leeches were frozen (-80°C)

for determination of body ammonia, while the integument of the anterior half was dissected (see tissue preparation) for gene expression analysis.

2.5 Body ammonia and urea content

Deproteinization of leech body tissue samples for ammonia/urea analysis was modified after Veauvy et al. (Veauvy et al., 2008) with the entire procedure performed on ice or in a refrigerated centrifuge. Diced frozen (-80°C) leeches were homogenized (Powermax AHS 200, VWR International, Radnor, PA, USA) in 10 volumes of ice cold 6% perchloric acid (assuming a 1 g ml^{-1} density of tissue). Homogenates were incubated on ice (10 mins) for deproteinization of the samples to occur. Homogenates were then centrifuged (5 mins, 4°C, 5000 x g) and the supernatant was neutralized with 0.6 volumes of 2.5 mol l^{-1} $KHCO_3$. Neutralized samples were centrifuged (5 mins, 4°C, 16000 x g) and immediately analyzed for ammonia (see ammonia and urea measurement).

Following deproteinization, body urea was analyzed using the colorimetric diacetyl monoxime/thiosemicarbazide assay (Rahmatullah and Boyde, 1980). In summary, one volume of neutralized body homogenate or urea standard was mixed with 0.5 volumes of urea assay reagent and incubated in a water bath (100°C, 10 mins). Cooled samples were spectrophotometrically (Abs_{540nm}) analyzed on a microplate reader (Powerwave, BioTek, Winooski, VT, USA). The composition of urea assay reagent was (in mol l^{-1}): 1.2 H_2SO_4, 0.33 H_3PO_4, $1.37x10^{-4}$ $FeCl_3$, $6.1x10^{-5}$ thiosemicarbazide, and $2.74x10^{-3}$ diacetylmonoxime. Urea standards (0, 20, 40, 80, 100, and 120 μmol l^{-1} urea) were prepared in deionized water.

2.6 Ammonia and urea measurement

Total ammonia was measured using a gas-sensitive NH_3 electrode (Thermo Orion, Beverly, MA, USA) connected to a digital pH meter as previously described in detail (Weihrauch et al., 1998). The electrode has a sensitivity capable of accounting for ± 1 μmol l^{-1} in the 4-50 μmol l^{-1} ammonia range and ± 1.5 μmol l^{-1} in the 50-200 μmol l^{-1} ammonia range. Measurement of total urea by the gas-sensitive NH_3 electrode was performed as described previously (Cruz et al., 2013). Briefly, prior to urease treatment (10 U ml^{-1}, 25°C, 30 mins) for the measurement of urea, the ammonia concentration of the samples was measured to determine the background ammonia in the sample. Total urea in urease-treated samples was calculated according to equation 1, where S_A is the sample total ammonia after urease treatment and S_B is the background ammonia prior to the urease treatment. Standard curves were prepared from the corresponding experimental solutions.

$$(equation\ 1)\ Urea = \frac{S_A - S_B}{2}$$

2.7 Na^+/K^+-ATPase activity

Na^+/K^+-ATPase activity of the leech skin was measured spectrophotometrically at 20°C based on established protocols (Gibbs and Somero, 1989; McCormick, 1993). The skin was homogenized in 15 volumes of ice-cold buffer containing (in mmol l^{-1}) 150 sucrose, 10 EDTA, 50 imidazole, and 0.1% (w/v) sodium deoxycholate, and subsequently centrifuged at 5000 x g for 1 min at 4°C. The assay procedure was the same as described previously (Cruz et al., 2013) with the exception of using 5 mmol l^{-1} ouabain for inhibiting the Na^+/K^+-ATPase in the current

study. Activities were determined using either 10 mmol l^{-1} KCl or 10 mmol l^{-1} NH_4Cl. Protein concentrations were determined using the Biuret assay using bovine serum albumin for standard curve preparation.

2.8 Whole animal sodium flux experiments

For sodium flux experiments, leeches acclimated to Edmonton tap water (containing 300 μmol l^{-1} Na^+, pH 8) were placed in culture flasks containing 40 ml dechlorinated Edmonton tap water. Sodium uptake was measured using radiolabeled $^{22}Na^+$ over a two-hour flux period. At the start of each flux, 0.1 μCi l^{-1} $^{22}Na^+$ and either 0.05% DMSO or EIPA (0.1, 1, 10, and 100 μmol l^{-1}) dissolved in 0.05% DMSO was added to the experimental chamber containing a single leech and given 5 mins to mix. After mixing, 5 ml water samples were collected at time 0 and 2 hours. Following the flux experiment, leeches were blotted dry and weighed. A 3 ml water sample was used for analyzing $^{22}Na^+$ radioactivity using a Gamma counter (Packard Cobra II, Auto Gamma, Model 5010, PerkinElmer, MA, USA), while the remaining 2 ml water sample was used for measuring total sodium with an atomic absorption spectrophotometer (PerkinElmer, Model 3300, CT, USA). Calculation of sodium uptake was done using equation 2, where Δcpm is the difference in $^{22}Na^+$ radioactivity at time 0 and 2 hours (cpm ml^{-1}), V is the volume of water during the flux period (ml), SA is the average specific activity measure at time 0 and 2 hours (cpm μmol^{-1} Na^+), t is the duration of the flux (hours), and m is mass of the leech (grams).

$$(equation\ \ 2)\ \ Na^{+}_{uptake} = \frac{\Delta cpm \times V}{SA \times t \times m}$$

2.9 Tissue preparation

In order to isolate the skin for RNA isolation, leeches were placed on ice for 20-30 minutes. The skin was dissected under RNase-free conditions by making a ventral incision from head to tail. Subsequently the dorsal skin was scraped from the internal organs and the muscle layers were removed by carefully scraping the skin with a scalpel until it became transparent. For body tissue samples, a dorsoventral cross section was taken in the middle of the leech to account for the majority of organs present. Dissected skin and body sections were stored in RNAlater (Applied Biosystems, Austin, TX, USA) at -80°C until RNA isolation.

2.10 Quantitative PCR

Total RNA was isolated from leech skin and the whole body with TRI Reagent (Sigma-Aldrich, St. Louis, MO, USA). Following phase separation, the RNA-containing phase was purified with E.Z.N.A. Tissue RNA Kit (Omega Bio Tek, Winooski, VT, USA) and spectrophotometrically quantified (NanoDrop 2000c, Thermo Scientific, Wilminton, DE, USA). Before synthesis of cDNA, 0.5 μg of total RNA was treated with DNase (DNase I, Invitrogen, Carlsbad, CA, USA) and purity was verified by PCR employing the primer pair No RPS2 F1/R1 (Table 1) targeting the ribosomal protein S2 (GenBank accession #: KM923910). Complementary DNA (cDNA) was synthesized from 0.5 μg DNase I-treated RNA using iScript cDNA synthesis kit (Bio-Rad, Mississauga, ON, CA). The cDNA quality was evaluated by PCR using the primer pair No RPS2 F1/R1 (Table 1). PCR products were assessed by ethidium bromide-stained agarose gel electrophoresis.

Partial sequences utilized as a base for designing species-specific primers to be employed in quantitative PCR were obtained through degenerate primers. Degenerate primers targeting the

Rh protein, V-ATPase (subunit B), Na^+/K^+-ATPase (α-subunit), and ribosomal protein S2 (Table 1) were designed based on conserved regions in published amino acid sequences of the respective genes. PCR products of the predicted size were purified (E.Z.N.A Gel Extraction Kit, Bio Tek, Winooski, VT, USA) and sequenced (Robarts Research Institute, London, ON, CA). A GenBank search with BLAST was used to verify the identity of the isolated PCR products. Primers for quantitative PCR were then generated using the obtained and verified sequences for the Rh protein, V-ATPase (subunit B), Na^+/K^+-ATPase (α-subunit), and ribosomal protein S2 (GenBank accession #: KM923907, KM923908, KM923909, and KM923910, respectively). For all primers utilized in qPCR (Table 1), a standard PCR was performed to verify the generation of a single PCR product of the predicted size.

For quantitative PCR (MiniOpticon, Biorad, Mississauga, ON, CA), standard curves were generated using a dilution series with known quantities of DNA (10^{+3}, 10^{+2}, 10^{+1}, 10^{+0}, 10^{-1}, 10^{-2} fg) from purified PCR products (E.Z.N.A Gel Extraction Kit, Bio Tek, Winooski, VT, USA) of the respective target genes. A minimum R^2 value of 0.98 was required for all standard curves. Quantitative PCR assays were performed with SsoFast EvaGreen Supermix (Biorad, Mississauga, ON, CA). A melt curve analysis was utilized to verify single PCR products following qPCR.

The ribosomal protein S2 served as the internal control for all mRNA expression experiments as it remained stable under all experimental conditions as tested by the NormFinder algorithm (Andersen et al., 2004) for both skin and body sections of *N. obscura*.

2.11 Molecular cloning and analysis of full length *N. obscura* Rhesus protein

To clone the full-length cDNA of the *N. obscura* Rh protein (NoRhp), a BLAST-verified partial sequence obtained through degenerate primers (Table 1) was utilized to design NoRhp specific primers to be used in RLM-RACE (FirstChoice RLM-RACE Kit, Ambion, Austin, TX, USA). 5' and 3' RLM-RACE products of the predicted size were cloned into pGEM T-easy vector (Promega, Madison, WI, USA) and sequenced (Robarts Research Institute, London, ON, CA). To obtain a proofread full-length cDNA of NoRhp, specific primers flanking the 5' and 3' of the open reading frame (ORF) were designed (Table 1). The proofread sequence was amplified utilizing Phusion High-Fidelity DNA Polymerase (Thermo Scientific, Ottawa, ON, CA) and sequenced (Robarts Research Institute, London, ON, CA). Alignment of NoRhp with published Rhesus proteins was performed by MUSCLE alignment of amino acid sequences on MEGA 5 (Tamura et al., 2011). Generation of predicted transmembrane domains was done with Phobius (Käll et al., 2004), TMHMM 2.0 (Krogh et al., 2001), and TMAP (Persson and Argos, 1994).

Table 1: Primers employed in amplification of NoRhp, V-ATPase B subunit, Na^+/K^+-ATPase α-subunit, and ribosomal protein S2. Primers employed in yeast expression contain restriction enzymes SpeI and XhoI in the primer name while all other primers containing the prefix "No" were utilized for quantitative PCR. Y, replaces C/T; N, replace A/T/G/C; R, replace A/G; D, replaces A/G/T.

Primer	Nucleotide sequence (5' → 3')	Annealing Temp. (ºC)	Product size (bp)
Rh-protein			
DegRh F2	CAYGCNTTYGGNGCNTAYTTY	50	467
DegRh R2	TTRTGNACNCCRCANGTRTCR	50	
NoRhp F1	TTTCAACTGTGCTTTGGCTG	60	283
NoRhp R1	GTTGCAACACGGAGTGAAGA	60	
NoRhp SpeI F	GTATAACTAGTGCGAGCATGGGTCTTACAGT	60	1491
NoRhp XhoI R	GTATACTCGAGTTATTAAGCATTGTTTTCGATCATGG	60	
H^+-ATPase			
HAT F2	GCNATGGGNGTNAAYATGGA	45	390
HAT R4	TGNGTDATRTCRTCGTTNGG	45	
No HAT F1	AATTTGGCCAATGATCCAAC	60	184
No HAT R1	AACCTCGTCTACCGGGAACT	60	
Na^+/K^+-ATPase			
NaK 10F	ATGACNGTNGCNCAYATGTGG	45	705
NaK 16R	GGRTGRTCNCCNGTNACCAT	45	
No NaK F1	ATGTACCGGTGCTGAAGAGG	60	289
No Nak R1	CTGCTCCATTCCTTGTCCAT	60	
RPS2			
Annelid RPS2 F1	AAGGAGTTYGARATCATTGATTTCT	50	448
Annelid RPS2 R1	TGGCRAAGTTGCCRAGRGTAG	50	
No RPS2 F1	GGGCGTTAAGTGCTCAAAAG	60	200
No RPS2 R1	CAACGATGCCAGTTCCTCTT	60	

2.12 Yeast complementation assays

The ORF of NoRhp cDNA (nt -6 to +1482, where +1 is A of the ATG start codon) was amplified (Phusion High-Fidelity DNA Polymerase, Thermo Scientific, Ottawa, ON, CA) using specific primers containing Spe I and Xho I restriction sites on the 5' and 3' ends, respectively. Amplified PCR products were then purified, digested, and ligated into the Spe I and Xho I restriction sites of the yeast expression vector pRS426-MET25.

The expression systems used in this study was *Saccharomyces cerevisiae* strains 23344c (ura3) (M. Grenson, unpublished) and 31019b (mep1Δ mep2Δ mep3Δ ura3) (Marini et al., 1997), which are isogenic with the wild type Σ1278b (Bechet et al., 1970). Transformation of yeast strains with expression vectors was achieved by heat shock as described previously (Gietz et al., 1992). Transformed yeast cells were grown in buffered minimal medium containing 3% glucose as a carbon source (Jacobs et al., 1980). The nitrogen sources used were 3 mmol l^{-1} $(NH_4)_2SO_4$ or 0.1% (6.8 mmol l^{-1}) glutamine. The yeast strain 31019b transformed with the Human RhCG was utilized as a positive control (Marini et al., 2000). Yeast cells transformed with NoRhp were verified for the correct insert by PCR on yeast colonies utilizing NoRhp qPCR primers (Table 1).

2.13 Phylogenetic analysis of Rhesus glycoproteins

The Rh protein data set contained 49 full-length cDNA sequences. Amino acid sequences of Rh protein data set were aligned by MUSCLE alignment in MEGA 5 (Tamura et al., 2011). Phylogenetic analysis of MUSCLE aligned sequences was done in MEGA 5 using maximum likelihood method with the Jones-Taylor-Thornton + four categories of gamma substitution rates + invariable sites model and Nearest Neighbor Interchange (NNI) Heuristic Method. Bootstrap

values were determined from 1000 bootstrap replicates. The maximum likelihood tree was rooted with the prokaryotic Rh protein from *Nitrosomonas europaea*.

2.14 Chemicals

Sodium thiosulfate, ammonium chloride, Tris hydrochloride, and MES were purchased from Fisher Scientific (Ottawa, ON, CA). All other chemicals (unless otherwise stated) were of analytical grade and purchased from Sigma-Aldrich (St. Louis, MO, USA).

2.15 Statistics

Data are presented as mean ± standard error of the means (SEM). All data were tested for homogeneity of variance with Levene's test and normal distribution with Shapiro-Wilk test. Differences between two means were tested with a Student's t-test, while differences between more than two means were tested with a one-way ANOVA. In the case that data were not normally distributed or did not show homogenous variance, non-parametric tests were used to assess statistical significance. When non-parametric tests were required, the Mann-Whitney test was used to determine differences between two means and Kruskal-Wallis test was utilized to assess differences between more than two means. P-values ≤ 0.05 were considered significant. Statistics employed in each experiment are also provided in the figure legends.

3. Results

3.1 Basics

Under control conditions, ammonia excretion rates in *Nephelopsis obscura* were 166.0 ± 8.6 nmol gFW^{-1} h^{-1} (n=96) and body ammonia content was 0.88 ± 0.06 μmol gFW^{-1} (n=12). Urea excretion rates were measured to 14.7 ± 1.9 nmol gFW^{-1} h^{-1} (n=29) and body urea content was 0.51 ± 0.05 μmol gFW^{-1} (n=12). Apically-directed ammonia production by theophylline-activated *N. obscura* skin mounted in an Ussing chamber was shown to maintain stable apically-directed metabolic excretion over three consecutive 1.5-hour time periods at 22.5 ± 0.8 nmol cm^{-2} h^{-1}, 21.1 ± 0.6 nmol cm^{-2} h^{-1}, and 19.9 ± 1.7 nmol cm^{-2} h^{-1} (n=5).

3.2 Transporter mRNA expression body vs. skin

Relative mRNA expression of NoRhp, V-ATPase, and Na^+/K^+-ATPase in skin and whole body sections of *N. obscura* revealed a 3-fold higher expression level of the Rh protein in the skin (Fig. 1). In addition, the Na^+/K^+-ATPase (α-subunit) also had, at least in tendency (p=0.07), a greater expression in the skin, while the V-ATPase (subunit B) was equally expressed (Fig. 1).

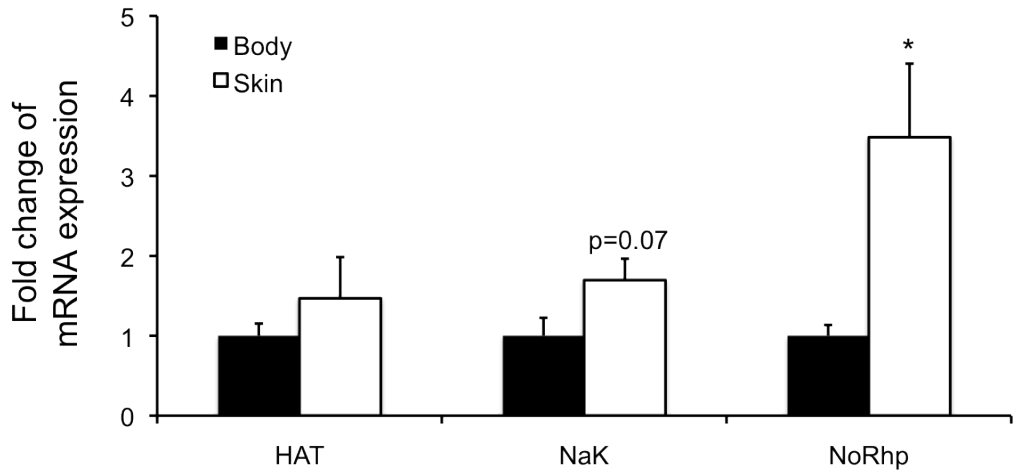

Figure 1: Relative mRNA expression levels of V-ATPase B subunit, Na^+/K^+-ATPase α-subunit, and NoRhp protein in the skin and whole body tissues of *N. obscura*. Gene expression levels were normalized utilizing the stable housekeeping gene, ribosomal protein S2. Data were standardized to whole body expression levels of the respective genes. Absolute expression levels of whole body tissue for V-ATPase, Na^+/K^+-ATPase, and NoRhp protein were respectively measured to 6.72 ± 1.5, 0.27 ± 0.05, and 0.14 ± 0.03 fg cDNA/5 ng total RNA. * denotes significant differences between body and skin mRNA expression levels (Mann-Whitney U test $p \leq 0.05$). Data are presented as mean ± SEM (n=6).

3.3 Ammonia excretion mechanism

Disruption of energy metabolism with 1 mmol l^{-1} sodium azide, an inhibitor of cytochrome c oxidase, as well as several other heme-containing proteins, reduced ammonia excretion by ca. 36% (Fig. 2). A similar inhibition was observed for the V-ATPase and carbonic anhydrase after the application of concanamycin C (0.005 mmol l^{-1}) and acetazolamide (1 mmol l^{-1}), respectively (Fig. 2).

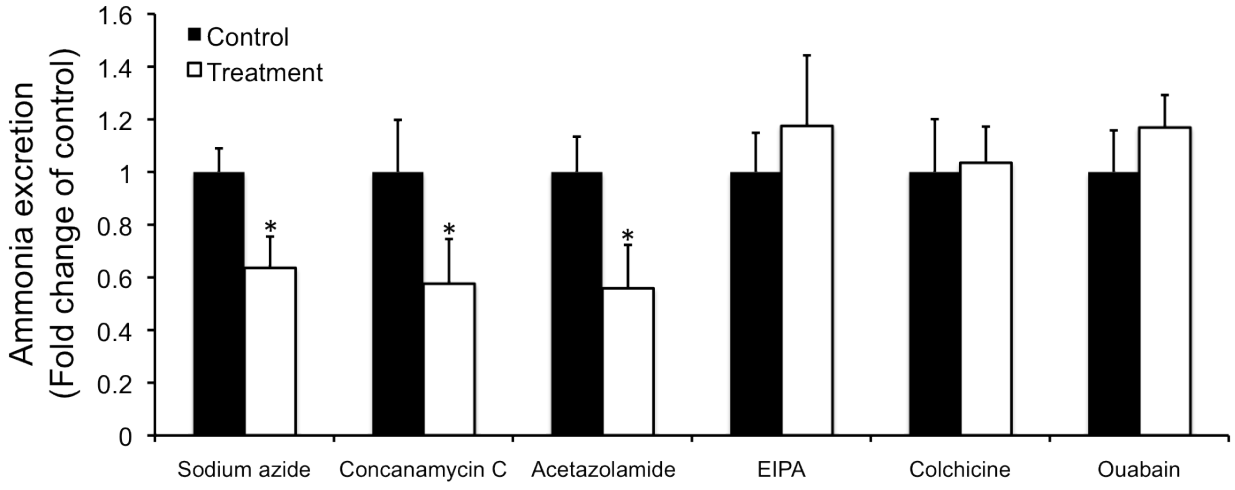

Figure 2: Effects of different pharmacological agents on ammonia excretion rates in *N. obscura*. Control excretion rates were standardized to 1, with excretion rates measured in the presence of pharmacological agents given as a fold-change relative to the respective control. Concentrations of pharmacological agents used were: 1 mmol l^{-1} sodium azide, 5 µmol l^{-1} concanamycin C, 1 mmol l^{-1} acetazolamide, 0.1 mmol l^{-1} EIPA, 5 mmol l^{-1} ouabain, and 2 mmol l^{-1} colchicine. * denotes significant differences from the controls (paired Student's t-test $p \leq 0.05$, prior to data standardizing). Data are presented as mean ± SEM (n=5-7). Experimental timeline is illustrated in appendix figure 15a.

Disruption of microtubule networks by colchicine (2 mmol l^{-1}) and inhibition of Na^+/H^+-exchangers by EIPA (0.1 mmol l^{-1}) resulted in no change in ammonia excretion (Fig. 2). In addition, $^{22}Na^+$ flux experiments demonstrated that the EIPA concentrations used are capable of effectively inhibiting sodium uptake by Na^+/H^+-exchangers (Fig. 3). Whole animal exposure to ouabain, an inhibitor of the Na^+/K^+-ATPase, did not affect ammonia excretion (Fig. 2). However, basolateral application of ouabain on theophylline-activated leech skin mounted in a modified Ussing chamber resulted in a 39% decrease in ammonia excretion (Fig. 4). Furthermore, an enzyme assay revealed that this pump accepts ammonium as a substrate. The assay confirmed that the ouabain-sensitive ATPase activity in the skin homogenates did not change whether ammonium (2.32 ± 0.13 nmol ADP min^{-1} mg $protein^{-1}$, n=4) or potassium was provided as a substrate (2.96 ± 0.37 nmol ADP min^{-1} mg $protein^{-1}$, n=4).

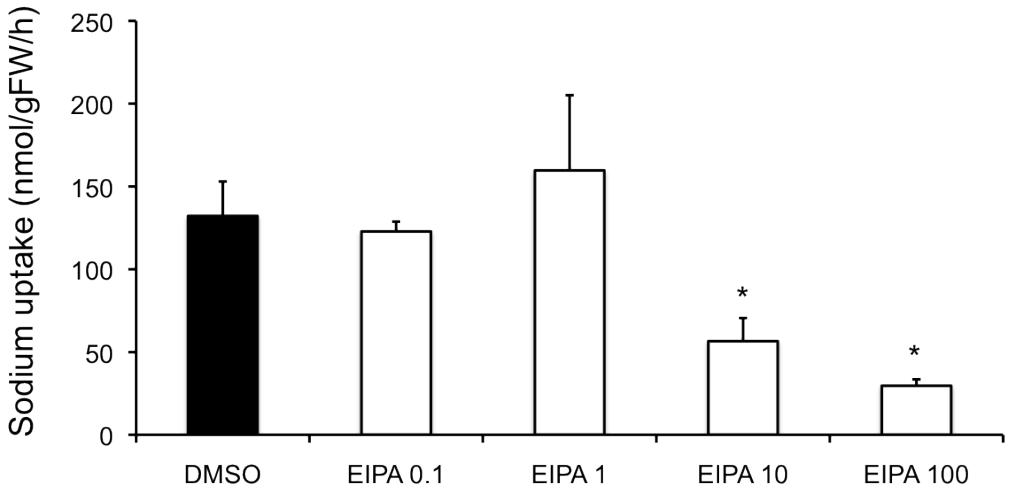

Figure 3: Dose-dependent sodium uptake rates in *N. obscura* exposed to increasing concentrations of EIPA dissolved in DMSO. Concentrations of inhibitor are given under each data point in μmol l^{-1}. * denotes significant differences from the DMSO control (unpaired Student's t-test $p \leq 0.05$). Data are presented as mean ± SEM (n=5-10).

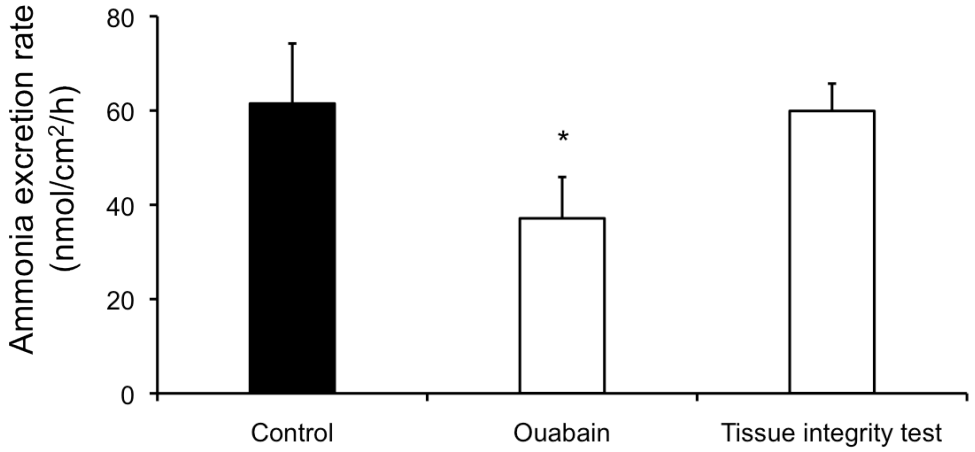

Figure 4: Effect of basolateral ouabain application on ammonia excretion rates of theophylline-activated *N. obscura* skin mounted in an Ussing chamber. An NH_4Cl gradient was applied across the tissue with 300 μmol l^{-1} on the basolateral side and no ammonia on the apical side. Control conditions were DTW enriched with 10 mmol l^{-1} theophylline on the apical side and leech Ringer's solution enriched with 300 μmol l^{-1} NH_4Cl, 10 mmol l^{-1} glucose, and 10 mmol l^{-1} theophylline on the basolateral side. Data presented in this graph are the difference between apically-excreted metabolic ammonia produced by the skin and the overall ammonia excretion toward the apical side. * denotes significant differences from the controls (repeated measures paired Student's t-test $p \leq 0.05$). Data are presented as mean ± SEM (n=6). Experimental timeline is illustrated in appendix figure 15b.

Ammonia excretion in *N. obscura* was highly dependent on environmental pH. When leeches were exposed to pH 5, ammonia excretion increased approximately 2-fold relative to the

control excretion rates (pH 8.3 unbuffered). Conversely, when leeches were exposed to high pH (pH 9.5 buffered), ammonia excretion rates decreased substantially to 13% of control levels (Fig. 5). Buffering of the control media with 5 mmol l^{-1} Tris and thus preventing the leech from manipulating the pH in its unstirred integumental boundary layer, did not affect the rate of ammonia excretion (Fig. 5).

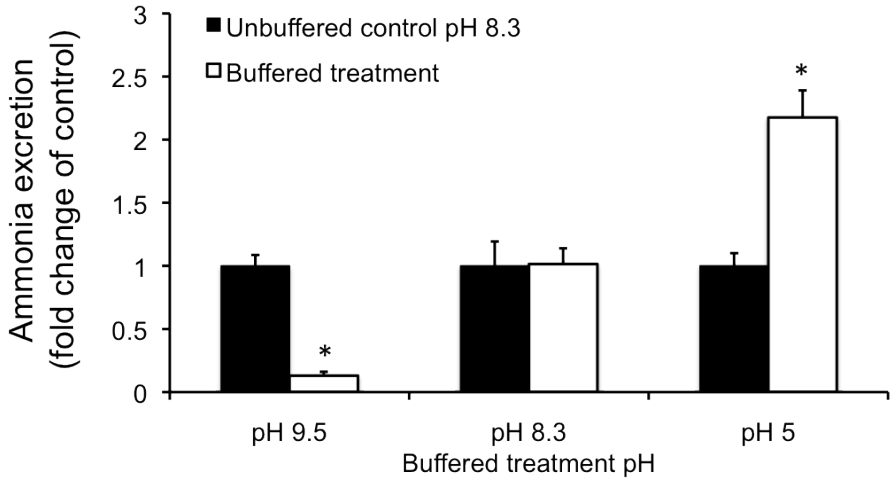

Figure 5: Effects of buffering dechlorinated tap water (DTW) to various pH regimes on ammonia excretion in *N. obscura*. Control excretion rates in unbuffered pH 8.3 DTW were standardized to 1, with excretion rates measured in buffered DTW given as a fold-change relative to the respective unbuffered control. * denotes significant differences from the unbuffered controls (paired Student's t-test $p \leq 0.05$, prior to data standardizing). Data are presented as mean ± SEM (n=6). Experimental timeline is illustrated in appendix figure 15c.

3.4 Identification and characterization of an Rhp protein in *N. obscura*

Employing isolated mRNA from skin tissues, degenerate primers, and subsequently the RACE technique, the full length (1482 bp) mRNA for a primitive Rh protein now named NoRhp (GenBank accession #: KM923907) was obtained.

Translation of the NoRhp ORF resulted in a 493 amino acid glycoprotein with a 49%, 46%, and 43% identity to verified ammonia transporters from trout (Rhbg, GenBank accession #: NP_001118134), human (RhCG, GenBank accession #: AAP81044) and pufferfish (Rhcg2,

GenBank accession #: BAE96344.1), respectively. Employing the Phobius (Käll et al., 2004), TMHMM 2.0 (Krogh et al., 2001), and TMAP (Persson and Argos, 1994) programs, a consensus of 11 transmembrane domains for NoRhp were predicted (Fig. 6). In addition, alignment of NoRhp with known ammonia-transporting Rh proteins from vertebrates (Marini et al., 2000; Nakada et al., 2007; Nawata et al., 2010a) and proposed ammonia-transporting Rh proteins of invertebrates (Martin et al., 2011; Weihrauch, 2006), demonstrated that the NoRhp contains the set of conserved amino acid residues crucial for conduction of ammonia transport (Zidi-Yahiaoui et al., 2009), with the exception of amino acid 266 in NoRhp, where now sits a leucine instead of isoleucine (Fig. 7). However, both amino acids bear non-polar alipathic residues. It was further predicted that the N-terminus of NoRhp is localized extracellularly and that the first intracellular loop contains three N-glycosylation sites: N53, N59, and N67 (Fig. 6).

To characterize NoRhp, a yeast functional complementation assay was conducted to determine the ammonia transport capability of NoRhp employing the *Saccharomyces cerevisiae* strain 31019b, which exhibits a growth deficiency in media with a sole nitrogen source of less than 5 mmol l^{-1} ammonia due to a deficiency of endogenous ammonia transporters (Marini et al., 1997). Complementation of this growth deficiency in the *S. cerevisiae* strain 31019b by expression of NoRhp and, as a positive control, human RhCG (Marini et al., 2000) demonstrates the ammonia transport capability of NoRhp protein when expressed in yeast (Fig. 8). In the positive growth control, all strains exhibited growth with 0.1% glutamine as a nitrogen source (Fig. 8).

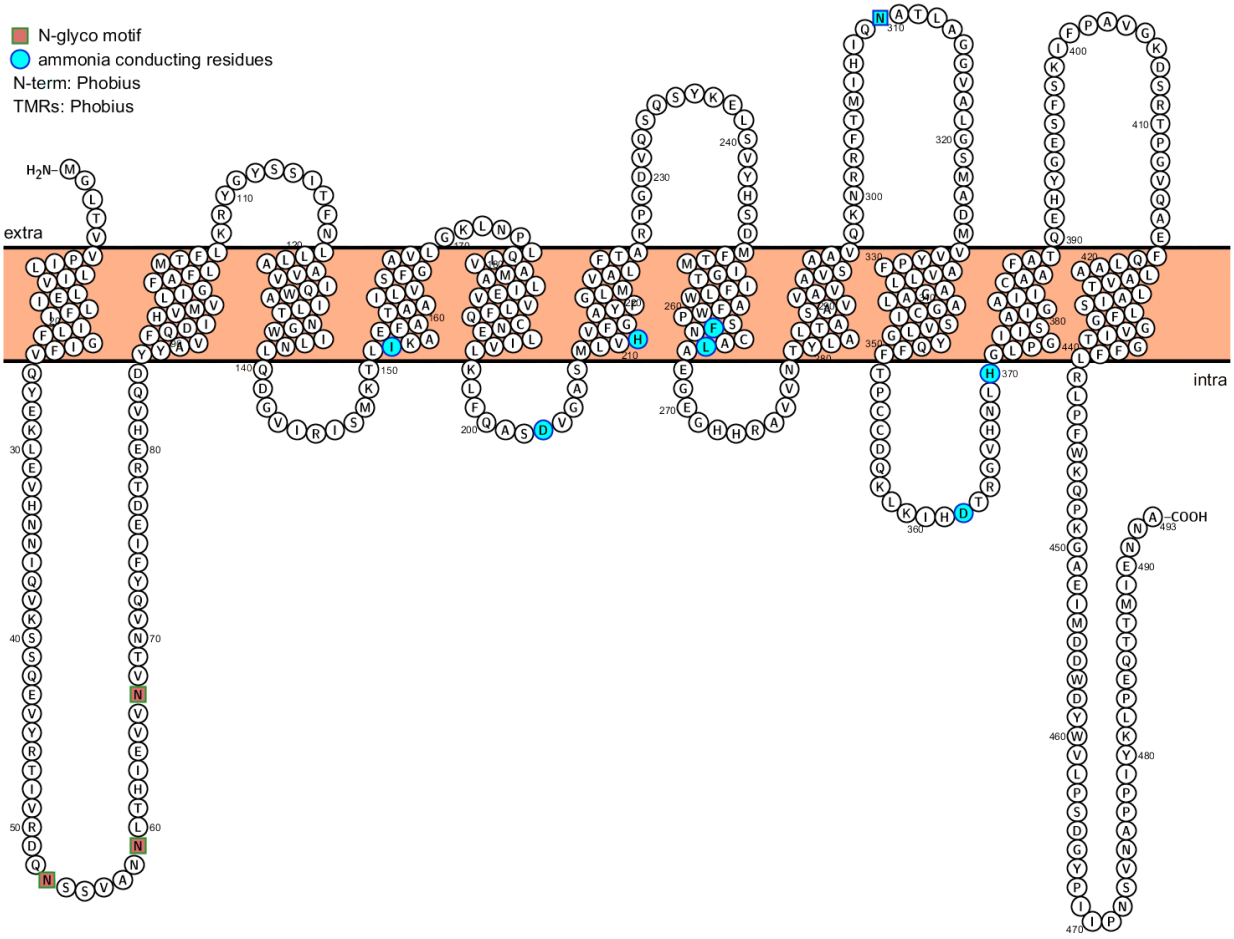

Figure 6: Localization of the predicted 11 transmembrane domains (Phobius) in the ammonia transporting NoRhp (GenBank accession #: KM923907) cloned from *N. obscura* skin tissue. Blocked residues indicate N-glycosylation sites and blue residues indicate ammonia conducting residues (Zidi-Yahiaoui et al., 2009).

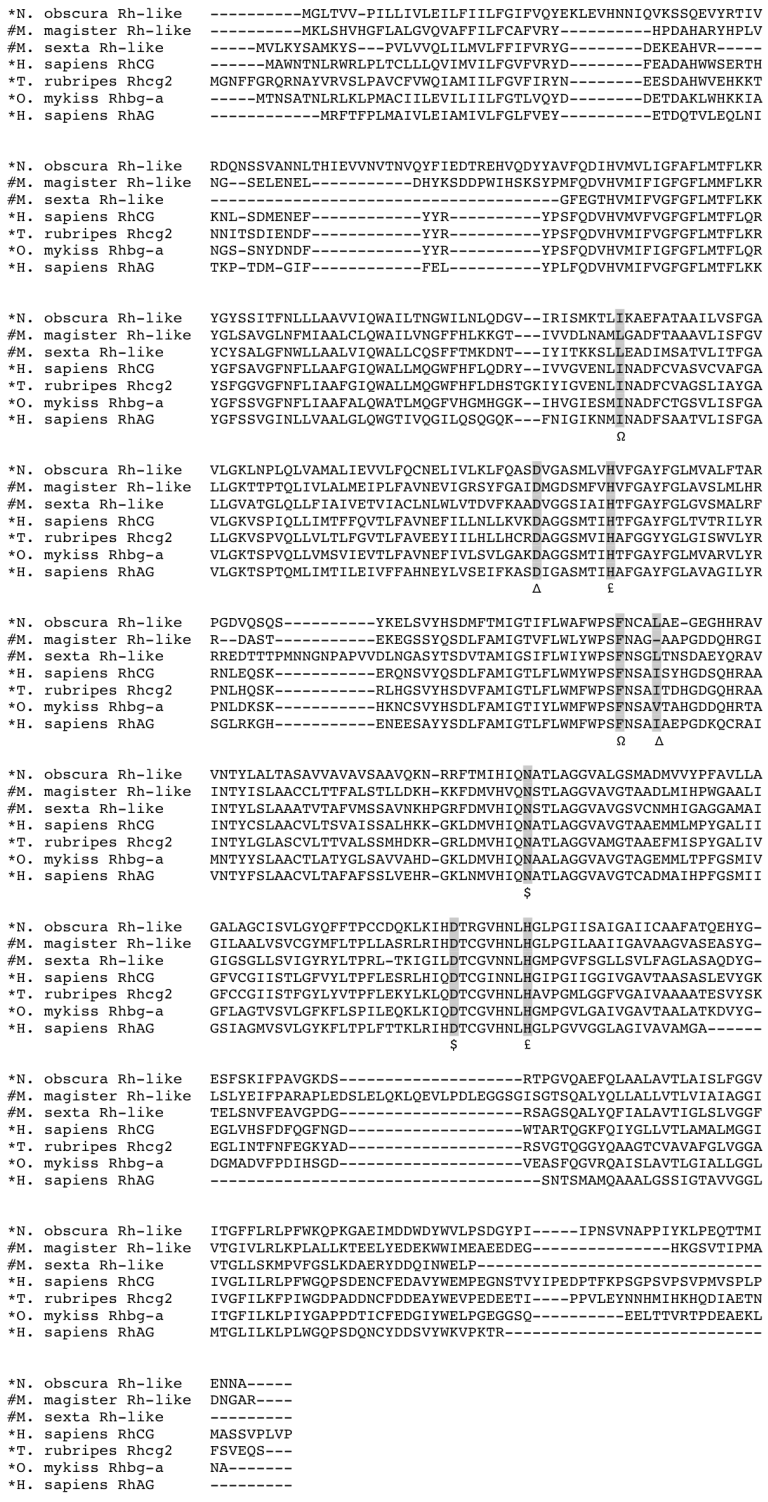

Figure 7: MUSCLE amino acid alignment of invertebrate Rhp and ammonia-transporting vertebrate Rh proteins. * denotes Rh proteins with verified ammonia transport capabilities, while # denotes Rh proteins with suggested role in ammonia transport. Ammonia-conducting residues are highlighted in grey. Ω indicates ammonia-conducting residues in the pore entrance, Δ indicates ammonia-conducting residues in the external vestibule, £ indicates ammonia-conducting residues in the pore center, and $ indicates ammonia-conducting residues in the internal vestibule (Khademi et al., 2004; Wu et al., 2010; Zidi-Yahiaoui et al., 2009).

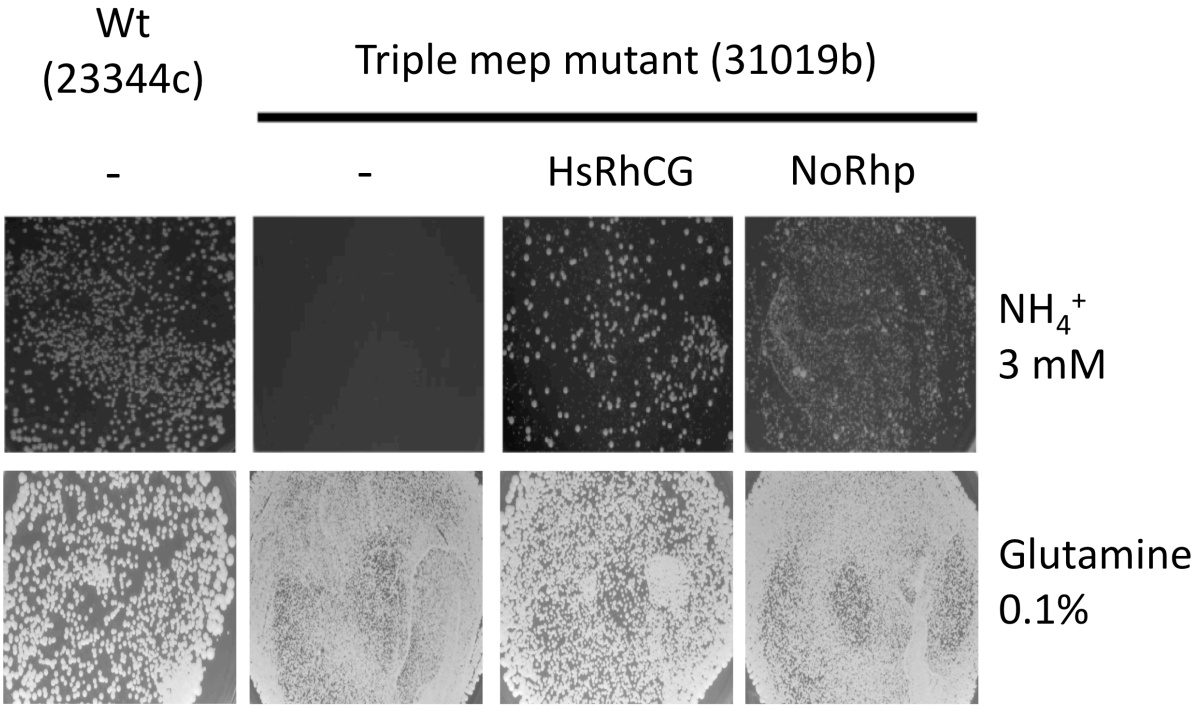

Figure 8: Yeast functional complementation assay on minimal media plates containing either 3 mmol l^{-1} $(NH_4)_2SO_4$ or 0.1% glutamine (positive growth control) as a sole nitrogen source. Wild type yeast cells (24433c) were transformed with an empty pRS426-MET25 yeast expression vector. Triple-*mep*Δ cells (31019b), deficient in the three endogenous Mep proteins, were transformed with either the empty pRS426-MET25 vector (negative control), or, with a pRS426-MET25 vector containing the open reading frame of the HsRhCG (positive control), or NoRhp genes.

3.5 Phylogenetic analysis of Rhesus glycoproteins

Reconstruction of MUSCLE-aligned Rh proteins utilizing Maximum Likelihood tree (ML-tree) method separated the 49 employed Rhesus proteins into five clear gene clusters, namely the vertebrate non-ammonia-transporting Rh30, the "primitive" invertebrate Rhp, and the three vertebrate ammonia-transporting gene clusters Rhag, Rhbg, and Rhcg (Fig. 9). The first node of the tree divides the Rh30s from the remaining gene clusters with a bootstrap value of 100 for the Rh30 cluster. Following divergence of the Rh30 proteins, the next gene cluster to

diverge is the primitive Rh proteins (Rhp), which do not clearly form a single group as demonstrated by the low bootstrap value (below 50). This divergence leaves the invertebrate Rhp proteins as a sister group to vertebrate ammonia-transporting Rh proteins (Rhag, Rhbg, and Rhcg), which have a bootstrap value of 99.

3.6 The effects of feeding

Feeding caused a significant increase in ammonia excretion rates (Fig. 10), but did not significantly increase urea excretion rates (data not shown). Ammonia excretion rates increased by 1.9-fold one hour after feeding and reached a peak excretion rate five hours after feeding (approximately 3-fold increase; Fig. 10). Interestingly, six hours after feeding, when expression rates were still elevated, relative mRNA expression levels of NoRhp, V-ATPase, and Na^+/K^+-ATPase in the skin remained unchanged when compared to controls (Fig. 11).

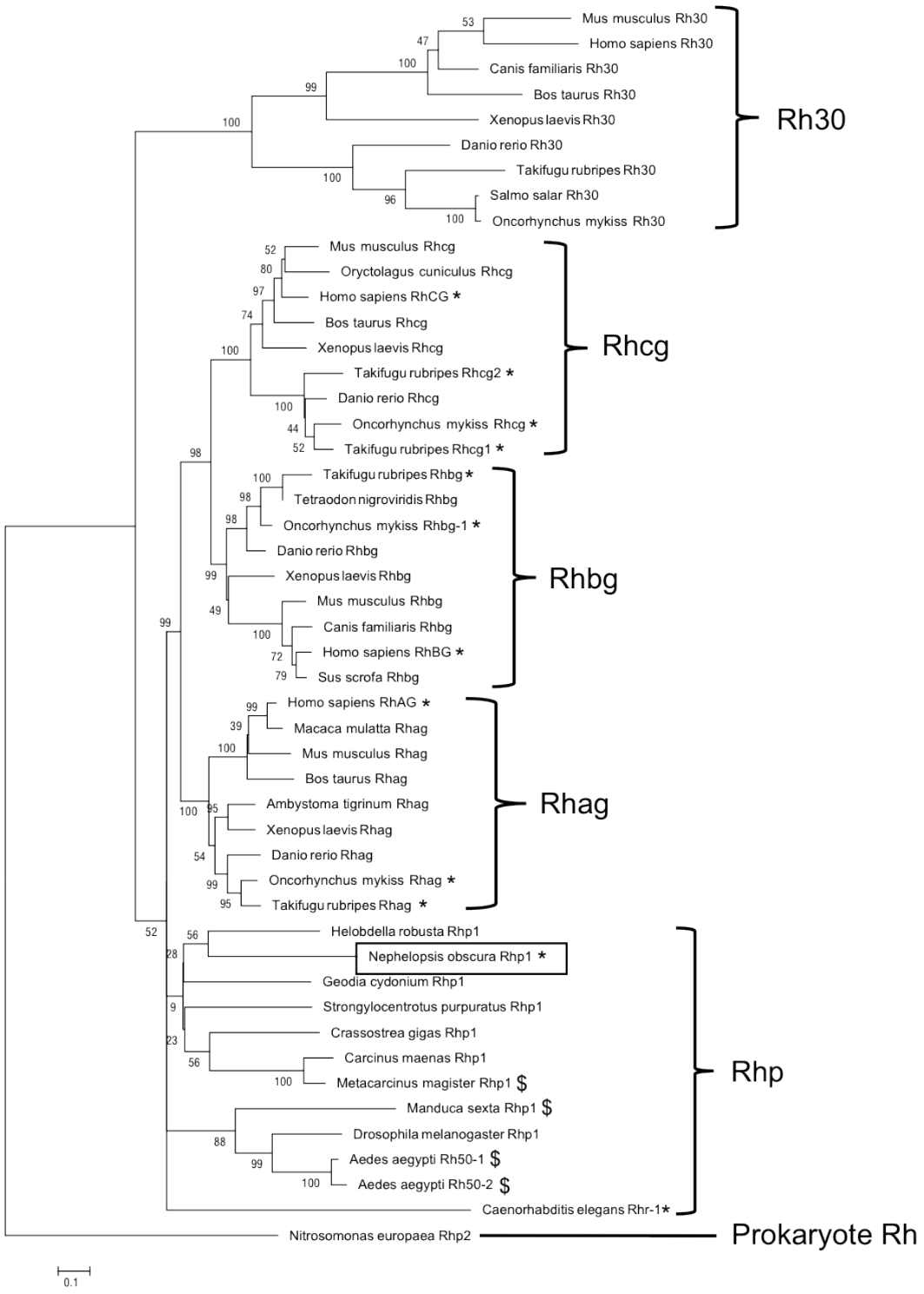

Figure 9: Maximum likelihood tree rooted employing the microbe *Nitrosomonas europaea* Rh protein as the outgroup. Numbers beside branches represent bootstrap values from 1000 replicates. The tree branches are drawn to scale, with the scale bar representing the number of amino acid substitutions per site. * denotes sequences with a confirmed ammonia transport capability and $ denotes invertebrate sequences with suggested ammonia transport capability. The black box indicates the sequence functionally characterized in this study as an ammonia transporter. GenBank accession numbers are given in the appendices Table 2.

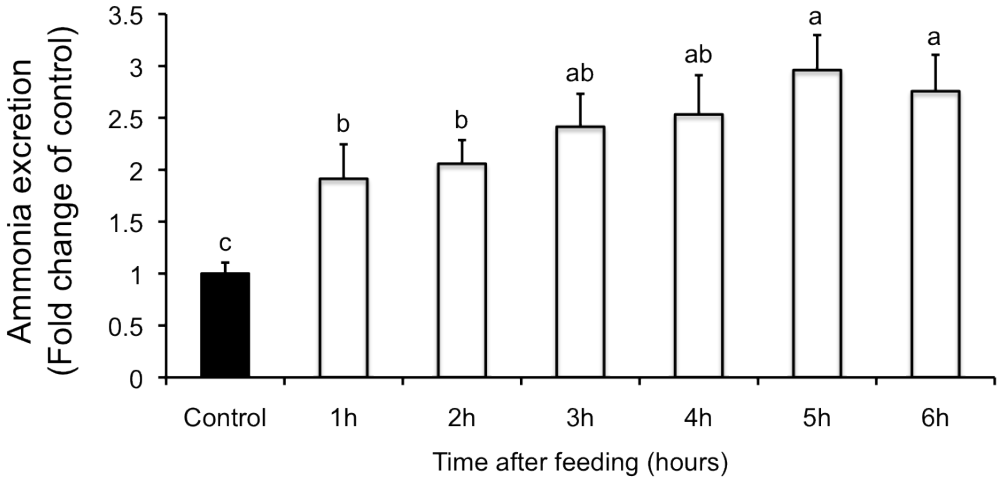

Figure 10: Ammonia excretion rates of *N. obscura* before (control) and after feeding. Ammonia excretion rates for six hours after feeding are shown. Means with the same letter are not significantly different. Data were analyzed with a repeated measures one-way ANOVA using a Tukey's pairwise comparison. Data are presented as mean ± SEM (n=6). Experimental timeline is illustrated in appendix figure 15d.

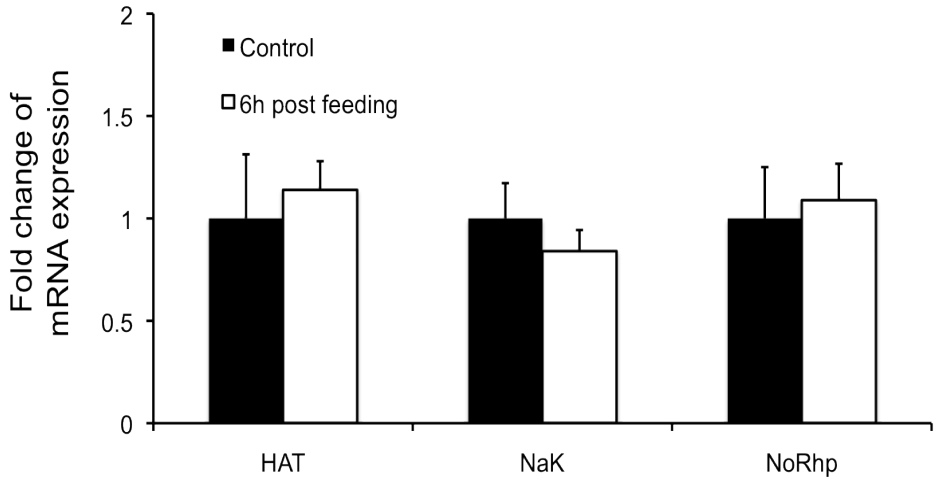

Figure 11: Relative mRNA expression levels of V-ATPase B subunit, Na^+/K^+-ATPase α-subunit, and NoRhp protein in the skin of control *N. obscura* and leeches six hours after feeding. Gene expression levels were normalized utilizing the ribosomal protein S2. Data were standardized to control skin expression levels of the respective genes. Absolute expression levels of control skin tissue for V-ATPase, Na^+/K^+-ATPase, and Rhp protein were measured to 3.25 ± 0.94, 1.2 ± 0.32, and 2.61 ± 0.61 fg cDNA/5 ng total RNA, respectively. Significant differences from control mRNA expression levels were analyzed using an unpaired Student's t-test $p \leq 0.05$. Data are presented as mean ± SEM (n=6).

3.7 The effect of high environmental ammonia (HEA) exposure

Short-term (1 hour) exposure of control leeches (DTW pH 8.3) to HEA (1 mmol l^{-1} NH_4Cl) led to elevated ammonia excretion rates (Fig. 12a). Upon returning control leeches to DTW, the rate of ammonia excretion decreased but remained elevated relative to the ammonia excretion rates in DTW prior to the HEA exposure (Fig. 12a). Following a one and seven-day acclimation to HEA, *N. obscura* demonstrated an ammonia excretion rate in DTW enriched with 1 mmol l^{-1} NH_4Cl equal to that of control leeches in DTW (Fig 12, b, and c). In animals acclimated for one day to HEA, ammonia excretion rates increased when transferred from high ammonia into DTW and were not different from control levels when re-exposed to DTW enriched with ammonia (Fig. 12b). In contrast, seven day acclimated leeches exhibited a significant increase in ammonia excretion rates when placed in DTW; however, re-exposure to DTW enriched with high ammonia led to an ammonia influx (Fig. 12c). In addition to changes seen in ammonia excretion with HEA exposure, long-term HEA exposure (1 mmol l^{-1} NH_4Cl) led to an increase in body ammonia levels from 0.88 ± 0.06 μmol gFW^{-1} (n=12) in control leeches to 2.31 ± 0.16 μmol gFW^{-1} (n=6) and 6.35 ± 0.24 μmol gFW^{-1} (n=6) in one and seven-day HEA acclimated leeches, respectively.

Moreover, a one-day exposure to HEA had no effect on the relative mRNA expression of NoRhp, V-ATPase B subunit, or Na^+/K^+-ATPase α-subunit in the skin (Fig. 13). However following a seven-day exposure to HEA, NoRhp was significantly down-regulated and Na^+/K^+-ATPase ($p=0.07$) was trending toward down-regulation (Fig. 13). As seen in one-day HEA acclimated leeches, seven-day HEA leeches showed no change in mRNA expression of V-ATPase B subunit (Fig. 13).

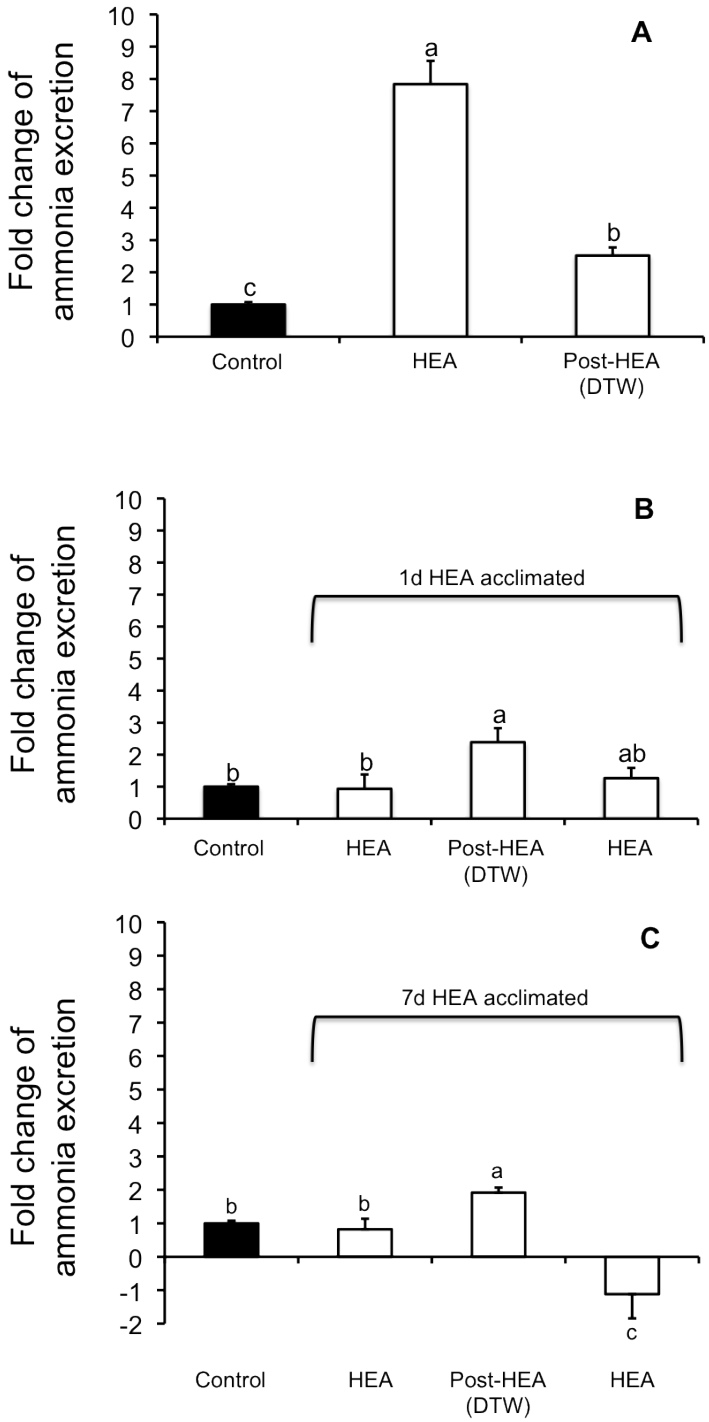

Figure 12: Effects of high environmental ammonia on ammonia excretion rates in *N. obscura*. **A.** Ammonia excretion rates of low ammonia (< 10 μmol l^{-1}) acclimated leeches in DTW (control), high environmental ammonia (1 mmol l^{-1}, HEA), and post-HEA exposure in DTW. **B.** Ammonia excretion rates of one-day HEA acclimated leeches in HEA, post-HEA in DTW, and re-exposure to HEA. **C** Ammonia excretion rates of seven-day HEA acclimated leeches in HEA, post-HEA in DTW, and re-exposure to HEA. Control excretion rates of low ammonia acclimated leeches were standardized to 1, with excretion rates measure in one-day and seven-day acclimated leeches given as a fold-change of the control excretion rate. Data were analyzed with a Kruskal-Wallis test $p \leq 0.05$. Data are presented as mean ± SEM (n=10-12). Experimental timeline is illustrated in appendix figure 15e.

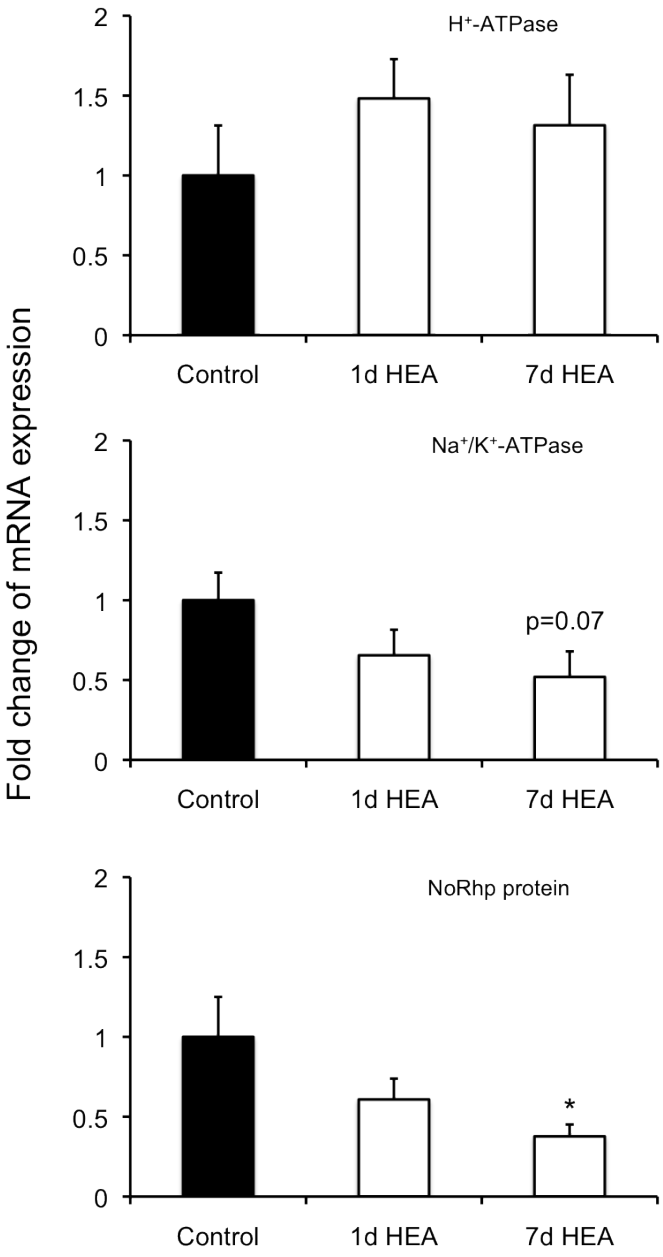

Figure 13: Relative mRNA expression levels of V-ATPase B subunit, Na^+/K^+-ATPase α-subunit, and NoRhp protein in the skin of control *N. obscura* and leeches acclimated to 1 mmol l^{-1} NH_4Cl for one and seven days. Gene expression levels were normalized utilizing the ribosomal protein S2. Data were standardized to control skin expression levels of the respective genes. Absolute expression levels of control skin tissue for V-ATPase, Na^+/K^+-ATPase, and Rhp protein were measured to 3.25 ± 0.94, 1.2 ± 0.32, and 2.61 ± 0.61 fg cDNA/5 ng total RNA, respectively. * denotes significant differences from control mRNA expression levels (unpaired Student's t-test $p \leq 0.05$). Data are presented as mean ± SEM (n=6).

4. Discussion

4.1 Basics

Based on measured body content and the excretion rates for both ammonia and urea, the carnivorous ribbon leech *Nephelopsis obscura* is ammonotelic, excreting 92% of the measured nitrogen as ammonia, similar to the closely related blood-feeding leech *Hirudo medicinalis* and other aquatic invertebrates (Larsen et al., 2014; Tschoerner and Zebe, 1989; Wright, 1995). While ammonia was the most abundantly excreted nitrogenous waste product measured, it must be noted that other nitrogenous waste products such as uric acid, guanine, allantoin, allantoic acid, or trimethylamine oxide (Bursell, 1967; Wright, 1995) have not been tested. Theophylline activated *N. obscura* skin mounted in an Ussing chamber generated a considerable amount of apically-released metabolic ammonia (about 20 nmol cm^{-2} h^{-1}), which is slightly higher but still comparable to that measured in frog skin where approximately 14 nmol cm^{-2} h^{-1} of apical release was measured (Cruz et al., 2013). It is important to note that in the frog skin study, the tissue was not activated by theophylline during the metabolic ammonia release experiment unlike in this study, which may account for the slight difference in metabolic ammonia release observed in the leech skin.

The observed ammonia transport capability of *N. obscura* skin mounted in an Ussing chamber (Fig. 4) and high mRNA expression levels of NoRhp and Na^+/K^+-ATPase (Fig. 1) in the leech skin relative to the rest of the body suggest that at least a portion of metabolically produced ammonia is excreted by this tissue. It should be noted that in Ussing chamber experiments, the tissue was theophylline-activated and concentrations of glucose and ammonia utilized in the study might not be at physiological levels as these levels are currently unknown for this leech. However, the experiment does demonstrate that the skin has a substantial capacity for ammonia

transport and may indeed be the main site of ammonia excretion. In terms of mRNA expression in skin vs. whole body, the lack of differential expression of the V-ATPase may be due to the importance of this protein in various physiological processes in different tissues throughout the body, whereas to our current knowledge, Rhesus proteins are limited to functioning in ammonia transport and potentially acid-base balance. While more thoroughly investigated for its role in water and salt balance, it cannot be excluded that the metanephridia (Wenning, 1996) and intestine (as shown for fish; Rubino et al., 2014), may also play a role in ammonia transport in leeches.

4. 2 Mechanism of ammonia excretion

Exposing the leeches to sodium azide, an inhibitor of the cytochrome c oxidase of the electron transport chain (Bennett et al., 1996), resulted in a decrease in ammonia excretion, potentially suggesting an active or secondary active mechanism of ammonia excretion. Conversely, sodium azide may also be affecting overall ammonia production due to a decrease in metabolic rate causing a reduced excretion rate. Therefore, these results should be interpreted with care as this inhibitor is capable of affecting various physiological processes, although it does provide circumstantial evidence for active ammonia excretion.

In terms of basolateral ammonia transport into the cytoplasm of the skin by Na^+/K^+-ATPase, the reduction of ammonia excretion in theophylline-activated leech skin in an Ussing chamber upon basolateral application of ouabain, demonstrates that Na^+/K^+-ATPase in leech skin plays a role in ammonia excretion. Furthermore, the fact that the Na^+/K^+-ATPase from leech skin does accept NH_4^+ as a substrate, as also observed for this enzyme in other ammonia-transporting

epithelia (Cruz et al., 2013; Nawata et al., 2010b; Towle and Hølleland, 1987), provides a strong indication that this pump contributes to a portion of ammonia entering the excretory epithelial cells.

The lack of inhibitory effects in whole animal ouabain experiments could be explained by poor diffusion of the inhibitor across the tight apical membrane or by studies investigating the "insect ouabain paradox", where it was suggested that OATPs (organic anion transporting polypeptide) co-localized with the Na^+/K^+-ATPase, actively excrete ouabain (Torrie et al., 2004). With the ouabain binding site in the Na^+/K^+-ATPase being localized at the intracellular end of ion permeation pathway (Sandtner et al., 2011), an active ouabain excretion would prevent this pharmacological agent from reaching the basolateral-localized Na^+/K^+-ATPase at inhibitory concentrations, thus creating the appearance of an ouabain insensitivity.

Ammonia excretion in *N. obscura* was dependent on ambient pH (Fig. 5), suggesting an ammonia-trapping mechanism by which NH_3 is transported from the epithelial cytoplasm into the apical unstirred boundary layer of the skin, likely mediated by the identified and functional NoRhp-protein. Cutaneous ammonia excretion via ammonia-trapping (also referred as acid-trapping) is a common excretion strategy in freshwater animals and has been shown for the planarian *S. mediterranea* (Weihrauch et al., 2012b), zebrafish larvae *D. rerio* (Shih et al., 2008), rainbow trout gills (Wilson et al., 1994), and the skin of the African clawed frog *X. laevis* (Cruz et al., 2013). An excretion mechanism by ammonia trapping over the skin is further supported by whole animal pharmacological evidence (Fig. 2) showing the involvement of the V-ATPase and carbonic anhydrase in this process. The data of the current study however, does not support the participation of a microtubule-dependent vesicular ammonia transport (Larsen et al., 2014) or Na^+/H^+-exchangers (NHEs). As seen in whole animal ouabain experiments, it is conceivable that

poor diffusion of colchicine across the tight apical membrane is responsible for the unaltered ammonia excretion in the presence of this inhibitor. In contrast, sodium flux data demonstrates that Na^+/H^+-exchangers were indeed inhibited in whole animal EIPA experiments, as sodium uptake is effectively decreased by this specific inhibitor at 100 μmol l^{-1} concentration, whereas ammonia excretion remained unaltered. Although not directly shown in this study, it can only be assumed that in *N. obscura*, the V-ATPase is localized in the apical membrane of the transport epithelium as shown for the skin and gills of various freshwater organisms (Klein et al., 1997; Lin et al., 2006; Wilson et al., 2000). Furthermore, while the carbonic anhydrase appears to play a role in ammonia excretion, likely by the generation of protons during CO_2 hydration, it remains unclear as to whether this occurs intracellularly or at the surface of the tissue via a membrane-bound carbonic anhydrase.

Interestingly, unlike as shown for the planarian *S. mediterranea* (Weihrauch et al., 2012b), rainbow trout *O. mykiss* (Rahaman-Noronha et al., 1996), and African clawed frog *X. laevis* (Cruz et al., 2013), buffering the environmental media to the pH of control non-buffered water did not affect ammonia excretion. This suggests that the leech may not be manipulating the pH of its unstirred boundary layer at the epithelial cell surface to promote ammonia trapping. However, the poorly ventilated crypts of the mucus-secreting glands embedded in the skin of leeches (Ahmed and Rahemo, 2013) could provide a microenvironment for the acidification of an unstirred boundary layer. Therefore, similar to the V-ATPase-bearing rhabdites in the planarians (Weihrauch et al., 2012b), it is likely that the V-ATPase is also abundant in the mucus-secreting cells of *N. obscura*. Future studies investigating the cellular localization of the V-ATPase in the skin of *N. obscura* could identify the site of the apical acidification and acid-trapping within the leech skin.

4.3 Characterization of *N. obscura* skin Rh protein, NoRhp

Members of the Rhesus protein family are found in various organisms from the microbe *Nitrosomonas europaea* to humans. Proteins of this family have been grouped into 6 gene clusters including Rhag, Rhbg, Rhcg, Rhp1, Rhp2, and Rh30. Of these 6 gene clusters, only one cluster, the Rhp1, is found in invertebrates, whereas the other five are found in vertebrates, with the Rhp2 being found only in non-mammalian vertebrates (Huang and Peng, 2005). However, Rhp2 proteins have not been characterized for localization and ammonia transport capabilities, respectively. In general, 12 transmembrane domains have been predicted for Rh-glycoproteins (Huang and Liu, 2001). Interestingly, an analyses of NoRhp (a primitive Rh protein) with Phobius (Käll et al., 2004), TMHMM 2.0 (Krogh et al., 2001), and TMAP (Persson and Argos, 1994) softwares, have predicted only 11 transmembrane domains for this functional transporter. It is possible that NoRhp actually contains 12 transmembrane domains as the softwares used only have 95-99% accuracy in predictions made, leaving room for error in predictions.

Phylogenetic analysis of the Rh protein family by reconstruction of maximum likelihood (ML) tree (Fig. 9) groups the Rhag, Rhbg, and Rhcg clusters closely together, while the Rhp group remains further away and the non-ammonia transporting Rh30 cluster being situated furthest away. The ML-tree positioning of the microbe *N. europaea* Rh protein, a member of the prokaryotic Rh proteins which are suggested to be the ancestral form from which eukaryotic Rh proteins were derived (Huang and Ye, 2010), implies that the primitive invertebrate Rhp-proteins are a sister group to the possibly more derived vertebrate ammonia-transporting Rhag, Rhbg, and Rhcg. While the ammonia-transporting capabilities of the vertebrate Rh proteins have received considerable attention (Weiner and Verlander, 2014), the role of Rhp genes in ammonia transport has been poorly studied. However, Rhp mRNA expression studies in the planarian *S.*

mediterranea (Weihrauch et al., 2012b), yellow fever mosquito *Aedes aegypti* (Weihrauch et al., 2012a), and Dungeness crab *Metacarcinus magister* (Martin et al., 2011) have demonstrated that these primitive Rh proteins do respond to ammonia stress.

Moreover, an amino acid alignment of the *NoRhp* with vertebrate Rh proteins demonstrated that amino acid residues critical for conducting ammonia transport in the human RhCG (Zidi-Yahiaoui et al., 2009) are also conserved in the *N. obscura* primitive Rh protein. This raised the question as to whether the NoRhp protein is also capable of ammonia transport. Indeed, the current study demonstrated clearly that NoRhp, the primitive Rh protein expressed in the skin of *N. obscura*, is capable of ammonia transport when expressed in yeast (Fig. 8). Beside CeRhr-1, the ubiquitously expressed Rh-protein in the soil nematode *Caenorhabditis elegans* (Adlimoghaddam, in press) and the Rh50s of the mosquito *Anopheles gambiae* (Pitts et al., 2014), *N. obscura* is now the third invertebrate where a protein in the "primitive Rh-protein" cluster has verified ammonia transport capabilities (Fig. 8). This underlines the notion that ammonia transport capabilities of Rh proteins may be an ancestral trait in the invertebrate Rh-protein (Rhp1 gene cluster) and the vertebrate ammonia-transporting Rh-protein (Rhag, Rhbg, and Rhcg) sister groups.

High mRNA expression levels of NoRhp in the skin and characterization of this protein as an ammonia transporter implicate NoRhp as a potential key transporter in the mechanism of cutaneous ammonia excretion in the leech. However, the cellular localization of NoRhp is not known to date. The obtained full open reading frame of NoRhp will help to develop antibodies for future localization studies necessary to gain clarity of the role of this transporter in the ammonia excretion mechanism in the skin and possibly other excretory sites in the leech.

4.4 The effects of feeding

Feeding resulted in a two to three-fold increase in ammonia excretion rates over 6 hours post-feeding (Fig. 10), likely due to an internal ammonia load caused by an increase in protein catabolism. This has previously been observed in the rainbow trout *O. mykiss*, where blood ammonia levels increased two to four hours after feeding (Bucking and Wood, 2008). However, in the current study, blood samples could not be taken to determine if blood ammonia levels were elevated after feeding. Unlike trout and planarians, where elevated ammonia excretion rates in response to feeding were paralleled with increased transcript levels of V-ATPase and Rh-protein (Weihrauch et al., 2012b; Zimmer et al., 2010), transcript levels of the Na^+/K^+-ATPase α-subunit, V-ATPase B-subunit, and NoRhp in *N. obscura* remained unchanged. Maximal excretion rates in *N. obscura* after feeding (approximately 3-fold increase) were comparatively low to that of trout and planarians. Therefore, one can only assume that the ammonia excretion machinery in the skin of the leech has the capacity to deal with moderately elevated ammonia loads potentially by activating the ammonia excretion mechanism using compounds such as cAMP, which has been shown to activate V-ATPase and Na^+/K^+-ATPase (Chibalins et al., 1992; Lowndes et al., 1990; Onken et al., 2000). However, it cannot be excluded that the metanephridial system or intestine, which have not been evaluated for differential mRNA expression levels, play a role in handling fluctuating ammonia levels in the body fluids.

4.5 Exposure to high environmental ammonia (HEA)

High environmental ammonia (HEA) poses a unique physiological stress in that outwardly directed ammonia gradients utilized for ammonia excretion by Rh proteins become

hampered. Under overwintering conditions, *N. obscura* in captivity have a tendency to aggregate in hiding spots (pers. observation), which may indicate a natural behavior of hiding under rocks or burrowing in the substrate in the wild. This behavior would expose leeches to conditions of poor ventilation, where the animals could potentially encounter high environmental ammonia as well as hypercapnia due to their own metabolic release of ammonia and CO_2.

In fish, short-term HEA exposure has been shown to cause ammonia influxes, as the animals were incapable of sufficient active excretion against the inwardly-directed ammonia gradient (Nawata et al., 2010b; Zimmer et al., 2010). Conversely, a short-term HEA exposure in *N. obscura* caused a large increase in ammonia excretion rates (Fig. 12a). This enhanced excretion in response to HEA could potentially be a result of a stress response, elevating metabolic rates. Elevation of metabolic rates would most likely result in a build up of endogenous ammonia, which could be used to reduce the strength of the inward ammonia gradient. Further, elevations in metabolic rate could result in elevated cAMP levels, which has been shown to activate both Na^+/K^+-ATPase (Chibalins et al., 1992; Lowndes et al., 1990) and V-ATPase (Onken et al., 2000). Activation of the V-ATPase and Na^+/K^+-ATPase could potentially stimulate the enhanced ammonia excretion observed during short-term HEA exposures in this study. In a comparable study, Dungeness crabs *Metacarcinus magister* were able to maintain an unaltered ammonia excretion across both anterior and posterior gills in the presence of HEA (Martin et al., 2011). It should be noted that these experiments on crabs were done on perfused gills; therefore, a possible ammonia excretion enhancement due to whole animal elevated metabolic rates cannot be excluded. While not possible in the present study, blood ammonia measurements would further clarify if elevated ammonia excretion rates were part of an activated ammonia excretion mechanism and/or due to establishment of elevated blood

ammonia (endogenous ammonia build-up) to counter the inward ammonia gradient. Following HEA stress, when animals were placed back in ammonia-free DTW, ammonia excretion began to decrease perhaps in an attempt re-establish control excretion rates (Fig. 12a), as also seen in the pufferfish *T. rubripes* (Nawata et al., 2010b).

One and seven-day HEA acclimated leeches, exhibited excretion rates similar to values observed in control animals when exposed to DTW enriched with 1 mmol l^{-1} ammonia (Fig. 12b and c). This is likely in part due to an elevation of blood and tissue ammonia, reducing the strength of the inwardly directed ammonia gradient. Reducing the strength of the inwardly directed P_{NH3} would allow for the active ammonia excretion mechanism to prevent uncontrolled ammonia influxes and most importantly the establishment of homeostasis. This proposed elevation of blood ammonia is further supported by the observed elevation in body ammonia levels in leeches acclimated to HEA, as well as the observed excretion rates when the animals were placed from ammonia-enriched DTW to ammonia-free DTW. If blood ammonia was not accumulated, exposure to ammonia-free water would have resulted in an ammonia excretion rate equal to that of control leeches. However, due to built up blood ammonia, this exposure allowed the strong outward ammonia gradient to drive an enhanced ammonia excretion in ammonia-free water. Similar results have been observed in HEA acclimated fish (Nawata et al., 2007; Nawata et al., 2010b), where recovery of control excretion rates coincided with elevations in blood ammonia.

Moreover, one-day HEA acclimated leeches appear to have maintained an uncompromised active ammonia excretion mechanism as mRNA expression of Na^+/K^+-ATPase α-subunit, V-ATPase B subunit, and NoRhp remained unchanged. While elevated blood ammonia may play a role in recovery of control excretion rates, one-day HEA acclimated

leeches appear to rely more heavily on the maintenance of their active ammonia excretion mechanism. This is evident as re-exposure to HEA resulted in the rapid re-establishment of control excretion rates, even though blood ammonia was likely lost during the ammonia-free water exposure. If ammonia excretion were solely dependent on elevated blood ammonia and less so on active ammonia excretion, then re-exposure to HEA would have resulted in ammonia influx.

In contrast, seven-day HEA acclimated leeches appeared to be more dependent on maintaining elevated blood ammonia levels for ammonia excretion, as re-exposure to HEA following a short exposure to ammonia-free water resulted in an ammonia influx. It is likely that the active mechanism of ammonia excretion has been depressed, as indicated by the reduced mRNA expression of Na^+/K^+-ATPase ($p=0.07$) and NoRhp. Therefore, in order to retain an ammonia efflux, leeches acclimated for seven days to HEA likely have elevated blood ammonia levels near or above environmental concentrations to promote a somewhat compromised active ammonia excretion. This notion is further supported by the observed 7-fold increase in body ammonia levels of long-term exposed leeches. It is also possible that down-regulation of Rh protein and tendency for down-regulation of Na^+/K^+-ATPase may be an attempt to prevent excessive blood ammonia loss, although the lack of change in the V-ATPase may be to maintain steady ammonia excretion across the apical membrane where the potential HEA threat interacts with the leech. Similar elevations of blood ammonia levels to near environmental levels have also previously been observed in decapod crabs and fish (Martin et al., 2011; Nawata et al., 2007; Nawata et al., 2010b).

In contrast to utilizing the skin for handling the evident environmental ammonia challenge, it is conceivable that alternative routes and/or mechanisms may be employed, which

include the metanephridia and intestine. Both of these tissues would not directly interact with the environmental media; therefore, inwardly directed ammonia gradients would not hamper the ability of these tissue to excrete ammonia as expected for the skin. Therefore, in seven-day HEA acclimated leeches, the observed down-regulation of NoRhp and Na^+/K^+-ATPase may be a result of active ammonia excretion in the skin shutting down and the intestine or metanephridia could be accounting for a portion of the observed ammonia excretion. In addition to alternative routes for ammonia excretion, it is plausible that other mechanisms are in play to reduce acute internal ammonia loads, such as elevation of glutamine synthetase activity to drive the conversion of ammonia into glutamine as seen in fish exposed to elevated environmental ammonia (Anderson et al., 2002). It is evident that further investigation into the role of the skin, intestine, and metanephridia under HEA conditions are required to clarify how the leech compensates for HEA. Future avenues of research in this topic include the use of isolated skin mounted in Ussing chambers to determine the capacity of active ammonia transport by this tissue following HEA acclimation. Further, evaluation of differential mRNA expression of the intestine and metanephridia following HEA acclimation could provide some indication as to whether either organ could be compensating for deficiencies in skin-mediated ammonia transport.

4.6 Hypothetical working model of active ammonia excretion in the skin of *N. obscura*

Due to the high expression of the functional NoRhp ammonia transporter in skin, whole animal pharmacology, and the demonstrated capacity for high ammonia transport rates by isolated leech skin, it can be strongly suggested that a portion of the overall body ammonia is excreted by the skin of *N. obscura*. According to the data obtained in this study, the Na^+/K^+-ATPase is responsible for a portion of blood ammonia transported into the cytoplasm of the

epithelial cells in the skin. In addition, Rh proteins in the skin may play a role in basal ammonia transport and, due to the suggested dual transport properties of Rh proteins, potentially CO_2 as well (Perry et al., 2010). On the apical side, the V-ATPase is thought to stimulate the generation of an outwardly directed P_{NH3}, driving NH_3 out of the cell via NoRhp by acidifying the unstirred mucus layer above the skin surface. However, based on the results of this study, it appears that unstirred boundary layer acidification may not be occurring at the surface of the epithelial cells. Therefore, it is hypothesized that acidification of the unstirred boundary layer may instead occur within the crypts of the mucus secreting cells, although future immunolocalization studies are required to strengthen this claim. Further, pharmacological data suggest that a cytoplasmic carbonic anhydrase may be providing protons to fuel the V-ATPase. Based on the results of this study, it cannot be concluded which cell type (epithelial cells and/or mucus secreting cells) in the skin of *N. obscura* is responsible for ammonia excretion, although it does provide strong evidence for ammonia excretion by the skin. In addition, future studies are required to demonstrate the localization of NoRhp in the skin as its location in the proposed model remains speculative. This described hypothetical model for ammonia excretion is illustrated in Fig. 13.

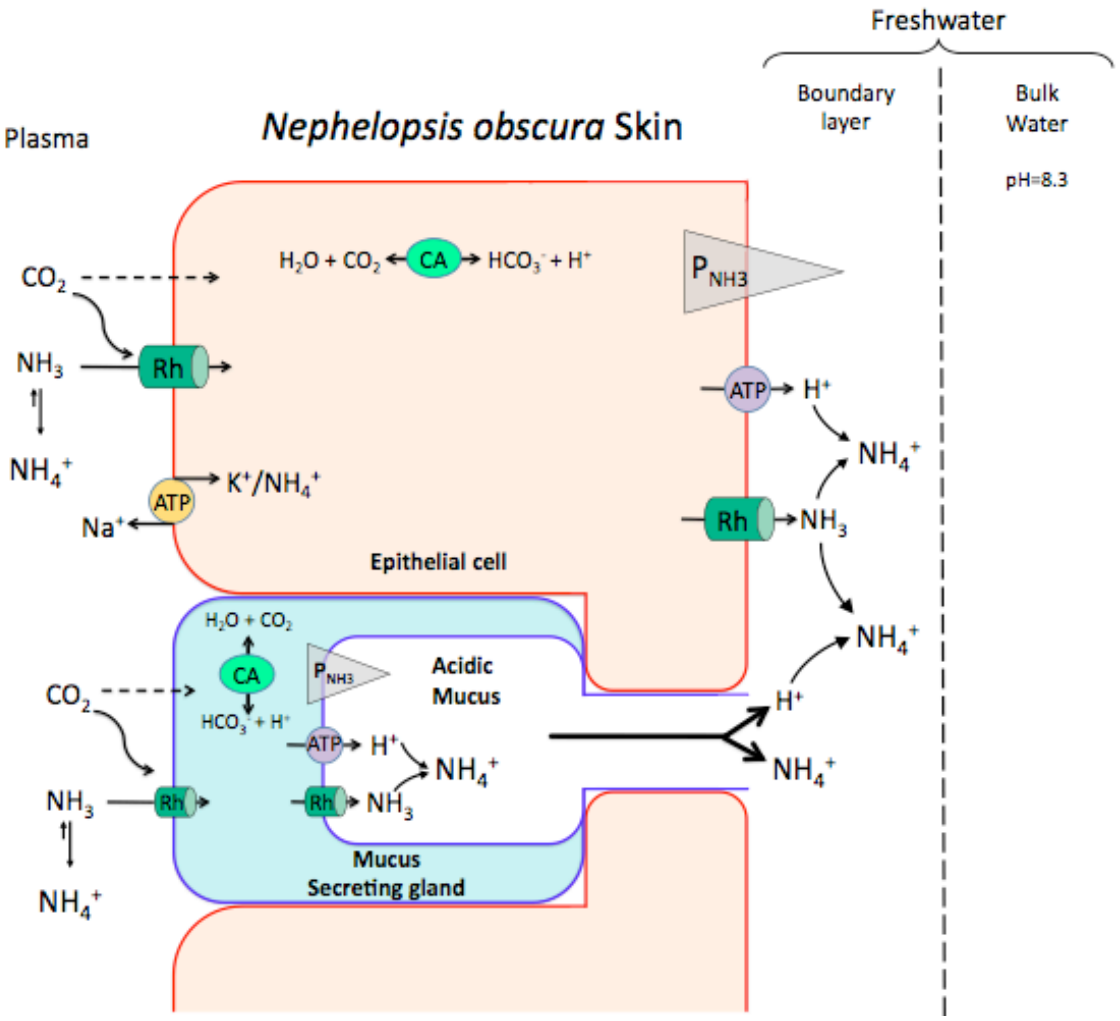

Figure 14: Proposed hypothetical model of active ammonia excretion across the skin of the ribbon leech *Nephelopsis obscura*. For a detailed description, refer to the text above.

5. Conclusion

This study provides a comprehensive investigation of the mechanism of ammonia excretion in a single member of the large and highly diverse group of freshwater invertebrates, where there is a paucity of mechanistic data. Utilizing the open reading frame of the identified

Rh protein from *N. obscura* (NoRhp), data were provided which further clarify the ammonia transport capability of primitive Rh proteins of invertebrates. The evidence provided for the ammonia transport capability of NoRhp and its higher expression in the skin of the leech, strongly suggests the skin as the likely site of ammonia excretion. The obtained data suggest a role of the Na^+/K^+-ATPase in transporting ammonia from the blood into the cytoplasm of the epithelial cells of the skin. In addition, the V-ATPase and indirectly also the carbonic anhydrase are likely involved in acidifying the unstirred boundary layer of the skin/crypts of skin (mucus). This in turn would generate a P_{NH3} over the apical membrane of the epithelial cells, driving NH_3 out of the cytoplasm through Rh proteins, possibly via NoRhp.

The ammonia excretion mechanism predicted for *N. obscura* shows many similarities to the mechanisms proposed for the gills of freshwater fish (Weihrauch et al., 2009; Wright and Wood, 2009), thereby suggesting an early evolution of the general freshwater ammonia excretion mechanisms.

6. References

Ahmed, S. T. and Rahemo, Z. I. F. (2013). Studies on the histology of the body wall of two species of leeches, Erpobdella octoculata and Haemopis sanguisuga (Annelida: Hirudinea). *Adv. J. Biol. Sci. Res.* **1**, 1–7.

Albrecht, J., Zielińska, M. and Norenberg, M. D. (2010). Glutamine as a mediator of ammonia neurotoxicity: A critical appraisal. *Biochem. Pharmacol.* **80**, 1303–1308.

Andersen, C. L., Jensen, J. L. and Ørntoft, T. F. (2004). Normalization of real-time quantitative reverse transcription-PCR data : a model-based variance estimation approach to identify genes suited for normalization , applied to bladder and colon cancer data sets. *Cancer Res.* **64**, 5245–5250.

Anderson, P. M., Broderius, M. A., Fong, K. C., Tsui, K. N. T., Chew, S. F. and Ip, Y. K. (2002). Glutamine synthetase expression in liver, muscle, stomach and intestine of Bostrichthys sinensis in response to exposure to a high exogenous ammonia concentration. *J. Exp. Biol.* **205**, 2053–2065.

Balian, E. V., Segers, H., Lévèque, C. and Martens, K. (2008). The freshwater animal diversity assessment: an overview of the results. In *Developments in Hydrobiologia*, pp. 627–637. Springer.

Bechet, J., Grenson, M. and Wiame, J. M. (1970). Mutations affecting the repressibility of arginine biosynthetic enzymes in Saccharomyces cerevisiae. *Eur. J. Biochem.* **12**, 31–39.

Bennett, M. C., Miady, G. W., Kwon, Y.-H. and Rose, G. M. (1996). Chronic in vivo sodium azide infusion induces selective and stable inhibition of cytochrome c oxidase. *J. Neurochem.* **66**, 2606–2611.

Binstock, L. and Lecar, H. (1969). Ammonium ion currents in the squid giant axon. *J. Gen. Physiol.* **53**, 342–361.

Braissant, O., McLin, V. A. and Cudalbu, C. (2013). Ammonia toxicity to the brain. *J. Inherit. Metab. Dis.* **36**, 595–612.

Bucking, C. and Wood, C. M. (2008). The alkaline tide and ammonia excretion after voluntary feeding in freshwater rainbow trout. *J. Exp. Biol.* **211**, 2533–2541.

Bursell, E. (1967). The excretion of nitrogen in insects. In *Advances in insect physiology*, pp. 33–67.

Cameron, J. N. and Heisler, N. (1983). Studies of ammonia in the rainbow trout: physico-chemical parameters, acid-base behaviour and respiratory clearance. *J. Exp. Biol.* **105**, 107–125.

Chan, H., Hazell, A. S., Desjardins, P. and Butterworth, R. F. (2000). Effects of ammonia on glutamate transporter (GLAST) protein and mRNA in cultured rat cortical astrocytes. *Neurochem. Int.* **37**, 243–248.

Chibalins, A. V, Vasiletss, L. A., Hennekess, H. and Geeringll, K. (1992). Phosphorylation of Na,K-ATPase α-subunits in microsomes and in homogenates of Xenopus oocytes resulting

from the stimulation of protein kinase A and protein kinase C *. *J. Biol. Chem.* **267**, 22378–22384.

Clauss, W. G. (2001). Epithelial transport and osmoregulation in annelids. *Can. J. Zool.* **79**, 192–203.

Cooper, A. J. L. and Plum, F. (1987). Biochemistry and physiology of brain ammonia. *Physiol. Rev.* **67**, 440–519.

Cruz, M. J., Sourial, M. M., Treberg, J. R., Fehsenfeld, S., Adlimoghaddam, A. and Weihrauch, D. (2013). Cutaneous nitrogen excretion in the African clawed frog Xenopus laevis: effects of high environmental ammonia (HEA). *Aquat. Toxicol.* **136-137**, 1–12.

Davies, R. W. (1973). The geographic distribution of freshwater Hirudinoidea in Canada. *Can. J. Zool.* **51**, 531–545.

Davies, W., Wrona, F. J. and Everett, R. P. (1978). A serological study of prey selection by Nephelopsis obscura Verrill (Hirudinoidea). *Can. J. Zool.* **56**, 587–591.

Dimski, D. S. (1994). Ammonia metabolism and the urea cycle: function and clinical implications. *J. Vet. Intern. Med.* **8**, 73–78.

Donini, A. and O'Donnell, M. J. (2005). Analysis of Na^+, Cl^-, K^+, H^+ and NH_4^+ concentration gradients adjacent to the surface of anal papillae of the mosquito Aedes aegypti: application of self-referencing ion-selective microelectrodes. *J. Exp. Biol.* **208**, 603–610.

Gibbs, A. and Somero, G. N. (1989). Pressure adaptation of Na^+/K^+-ATPase in gills of marine teleots. *J. Exp. Biol.* **143**, 475–492.

Gietz, D., St. Jean, A., Woods, R. A. and Schiestl, R. H. (1992). Improved method for high efficiency transformation of intact yeast cells. *Nucleic Acids Res.* **20**, 1425.

Harris, R., Coley, S., Collins, S. and McCabe, R. (2001). Ammonia uptake and its effects on ionoregulation in the freshwater crayfish Pacifastacus leniusculus (Dana). *J. Comp. Physiol. B Biochem. Syst. Environ. Physiol.* **171**, 681–693.

Huang, C. H. and Liu, P. Z. (2001). New insights into the Rh superfamily of genes and proteins in erythroid cells and nonerythroid tissues. *Blood Cells. Mol. Dis.* **27**, 90–101.

Huang, C. and Peng, J. (2005). Evolutionary conservation and diversification. *Proc. Natl. Acad. Sci.* **102**, 15512–15517.

Huang, C.-H. and Ye, M. (2010). The Rh protein family: gene evolution, membrane biology, and disease association. *Cell. Mol. life Sci.* **67**, 1203–1218.

Jacobs, P., Jauniaux, J.-C. and Grenson, M. (1980). A cis-dominant regulatory mutation linked to the argB-argC gene cluster in Saccharomyces cerevisiae. *J. Mol. Biol.* **139**, 691–704.

Käll, L., Krogh, A. and Sonnhammer, E. L. L. (2004). A combined transmembrane topology and signal peptide prediction method. *J. Mol. Biol.* **338**, 1027–1036.

Khademi, S., O'Connell III, J., Remis, J., Robles-Colmenares, Y., Miercke, L. J. W. and Stroud, R. M. (2004). Mechanism of ammonia transport by Amt/MEP/Rh: structure of AmtB at 1.35 A. *Science (80-.).* **305**, 1587–1594.

Klein, U., Timme, M., Zeiske, W. and Ehrenfeld, J. (1997). The H^+ pump in frog skin (Rana esculenta): Identification and localization of a V-ATPase. *J. Membr. Biol.* **157**, 117–126.

Knecht, K., Michalak, a, Rose, C., Rothstein, J. . and Butterworth, R. . (1997). Decreased glutamate transporter (GLT-1) expression in frontal cortex of rats with acute liver failure. *Neurosci. Lett.* **229**, 201–203.

Kormanik, G. A. and Cameron, J. N. (1981). Ammonia excretion in the seawater blue crab (Callinectes sapidus) occurs by diffusion, and not Na^+/NH_4^+ exchange. *J. Comp. Physiol.* **141**, 457–462.

Krogh, A., Larsson, B., von Heijne, G. and Sonnhammer, E. L. (2001). Predicting transmembrane protein topology with a hidden Markov model: Application to complete genomes. *J. Mol. Biol.* **305**, 567–580.

Kulkarni, G., Kulkarni, V. and Rao, A. B. (1989). Nephridial excretion of ammonia and urea in the freshwater leech, Poecilobdella viridis as a function of temperature and photoperiod. *Proc. Indian Natn. Acad.* **B55**, 345–352.

Larsen, E. H., Deaton, L. E., Onken, H., O'Donnell, M., Grosell, M., Dantzler, W. H. and Weihrauch, D. (2014). Osmoregulation and excretion. *Compr. Physiol.* **4**, 405–573.

Lin, B. Y. H. and Randall, D. (1991). Evidence for the presence of an electrogenic proton pump on the trout gill epithelium. *J. Exp. Biol.* **161**, 119–134.

Lin, L.-Y., Horng, J.-L., Kunkel, J. G. and Hwang, P.-P. (2006). Proton pump-rich cell secretes acid in skin of zebrafish larvae. *Am. J. Physiol. Cell Physiol.* **290**, C371–C3788.

Lowndes, J. M., Hokin-Neaverson, M. and Bertics, P. (1990). Kinetics of phosphorylation of Na^+/K^+-ATPase by protein kinase C. *Biochim. Biophys. Acta* **1052**, 143–151.

Lutz, P. and Siddiq, A. H. (1971). Nonprotein nitrogenous composition of the protonephridial fluid of the trematode Fasciola gigantica. *Comp. Biochem. Physiol.* **40A**, 453–457.

Marcaida, G., Felipo, V., Hermenegildo, C., Miñana, M.-D. and Grisolia, S. (1992). Acute ammonia toxicity is mediated by the NMDA type of glutamate receptors. *Fed. Eur. Biochem. Soc. Lett.* **296**, 67–68.

Marini, A. M., Vissers, S., Andre, B., Vissers, S. and Andre, B. (1997). A family of ammonium transporters in Saccharomyces cerevisiae. *Mol. Cell. Biol.* **17**, 4282–4293.

Marini, A., Matassi, G., Raynal, V., André, B., Cartron, J. and Chérif-zahar, B. (2000). The human Rhesus-associated RhAG protein and a kidney homologue promote ammonium transport in yeast. *Nat. Genet.* **26**, 341–344.

Marshall, W. S. (2002). Na(+), Cl(-), Ca(2+) and Zn(2+) transport by fish gills: retrospective review and prospective synthesis. *J. Exp. Zool.* **293**, 264–283.

Martin, M., Fehsenfeld, S., Sourial, M. M. and Weihrauch, D. (2011). Effects of high environmental ammonia on branchial ammonia excretion rates and tissue Rh-protein mRNA expression levels in seawater acclimated Dungeness crab Metacarcinus magister. *Comp. Biochem. Physiol. A. Mol. Integr. Physiol.* **160**, 267–277.

McCormick, S. D. (1993). Methods for nonlethal gill biopsy and measurment of Na^+,K^+-ATPase activity. *Can. J. Fish. Aquat. Sci.* **50**, 656–658.

Meijer, A. J., Lamers, W. H. and Chamuleau, R. A. F. M. (1990). Nitrogen metabolism and ornithine cycle function. *Physiol. Rev.* **70**, 701–748.

Nakada, T., Westhoff, C. M., Kato, A. and Hirose, S. (2007). Ammonia secretion from fish gill depends on a set of Rh glycoproteins. *FASEB J.* **21**, 1067–1074.

Nakhoul, N. L., Hering-smith, K. S., Abdulnour-nakhoul, S. M. and Hamm, L. L. (2001). Ammonium interaction with the epithelial sodium channel. *Am. J. Physiol. Renal Physiol.* **281**, 493–502.

Nawata, C. M., Hung, C. C. Y., Tsui, T. K. N., Wilson, J. M., Wright, P. a and Wood, C. M. (2007). Ammonia excretion in rainbow trout (Oncorhynchus mykiss): evidence for Rh glycoprotein and H^+-ATPase involvement. *Physiol. Genomics* **31**, 463–474.

Nawata, C. M., Wood, C. M. and O'Donnell, M. J. (2010a). Functional characterization of Rhesus glycoproteins from an ammoniotelic teleost, the rainbow trout, using oocyte expression and SIET analysis. *J. Exp. Biol.* **213**, 1049–1059.

Nawata, C. M., Hirose, S., Nakada, T., Wood, C. M. and Kato, A. (2010b). Rh glycoprotein expression is modulated in pufferfish (Takifugu rubripes) during high environmental ammonia exposure. *J. Exp. Biol.* **213**, 3150–3160.

Norenberg, M. D., Huo, Z., Neary, J. T. and Roig-Cantesan, A. (1997). The glial glutamate transporter in hyperammonemia and hepatic encephalopathy: Relation to energy metabolism and glutamatergic neurotransmission. *Glia* **21**, 124–133.

O'Donnell, M. J. (1997). Mechanisms of excretion and ion transport in invertebrates. In *Comparative Physiology* (ed. Dantzler, W. H.), pp. 1207–1289. New York: Oxford University Press.

Onken, H., Schöbel, A., Kraft, J. A. N. and Putzenlechner, M. A. X. (2000). Active NaCl absorption across split lamellae of posterior gills of the Chinese crab Eriocheir Sinensis: Stimulation by eyestalk extract. *J. Exp. Biol.* **203**, 1373–1381.

Parks, S. K., Tresguerres, M. and Goss, G. G. (2008). Theoretical considerations underlying Na(+) uptake mechanisms in freshwater fishes. *Comp. Biochem. Physiol. C. Toxicol. Pharmacol.* **148**, 411–418.

Perry, S. F., Braun, M. H., Noland, M., Dawdy, J. and Walsh, P. J. (2010). Do zebrafish Rh proteins act as dual ammonia-CO_2 channels? *J. Exp. Zool. A. Ecol. Genet. Physiol.* **313**, 618–621.

Persson, B. and Argos, P. (1994). Prediction of transmembrane segments in proteins utilising multiple sequence alignments. *J. Mol. Biol.* **237**, 182–192.

Pitts, R. J., Derryberry, S. L., Pulous, F. E. and Zwiebel, L. J. (2014). Antennal-expressed ammonium transporters in the malaria vector mosquito Anopheles gambiae. *PLoS One* **9**, e111858.

Rahaman-Noronha, E., Donnell, M. J. O., Pilley, C. M. and Wright, P. A. (1996). Excretion and distribution of ammonia and the influence of boundary layer acidification in embryonic rainbow trout (Oncorhynchus mykiss). *J. Exp. Biol.* **199**, 2713–2723.

Rahmatullah, M. and Boyde, T. R. C. (1980). Improvements in the determination of urea using diacetyl monoxime; methods with and without deproteinisation. *Clin. Chim. Acta* **107**, 3–9.

Rubino, J. G., Zimmer, A. M. and Wood, C. M. (2014). Intestinal ammonia transport in freshwater and seawater acclimated rainbow trout (Oncorhynchus mykiss): Evidence for a Na(+) coupled uptake mechanism. *Comp. Biochem. Physiol. A. Mol. Integr. Physiol.* **183C**, 45–56.

Sandtner, W., Egwolf, B., Khalili-Araghi, F., Sánchez-Rodríguez, J. E., Roux, B., Bezanilla, F. and Holmgren, M. (2011). Ouabain binding site in a functioning Na^+/K^+ ATPase. *J. Biol. Chem.* **286**, 38177–83.

Shih, T.-H., Horng, J.-L., Hwang, P.-P. and Lin, L.-Y. (2008). Ammonia excretion by the skin of zebrafish (Danio rerio) larvae. *Am. J. Physiol. Cell Physiol.* **295**, C1625–C1632.

Tamura, K., Peterson, D., Peterson, N., Stecher, G., Nei, M. and Kumar, S. (2011). MEGA5: molecular evolutionary genetics analysis using maximum likelihood, evolutionary distance, and maximum parsimony methods. *Mol. Biol. Evol.* **28**, 2731–2739.

Tian, J., Iwasaki, T. and Friesen, W. O. (2007). Muscle function in animal movement: passive mechanical properties of leech muscle. *J. Comp. Physiol. A. Neuroethol. Sens. Neural. Behav. Physiol.* **193**, 1205–1219.

Torrie, L. S., Radford, J. C., Southall, T. D., Kean, L., Dinsmore, A. J., Davies, S. a and Dow, J. a T. (2004). Resolution of the insect ouabain paradox. *Proc. Natl. Acad. Sci. U. S. A.* **101**, 13689–13693.

Towle, D. W. and Hølleland, T. (1987). Ammonium ion substitutes for K^+ in ATP-dependent Na^+ transport by basolateral membrane vesicles. *Am. J. Physiol. Regul. Integr. Comp. Physiol.* **252**, 479–489.

Tschoerner, P. and Zebe, E. (1989). Ammonia formation in the medicinal leech, Hirudo medicinalis-in vivo and in vitro investigations. *Comp. Biochem. Physiol.* **94A**, 187–194.

Veauvy, C. M., Walsh, P. J. and McDonald, M. D. (2008). Effect of elevated ammonia on tissue nitrogen metabolites in the ureotelic gulf toadfish (Opsanus beta) and the ammoniotelic midshipman (Porichthys notatus). *Physiol. Biochem. Zool.* **82**, 345–352.

Wall, S. M. and Koger, L. M. (1994). NH4+ transport mediated by Na^+-K^+-ATPase in rat inner medullary collecting duct. *Am. J. Physiol.* **267**, F660–F670.

Weber, W., Dannenmaier, B. and Clauss, W. (1993). Ion transport across leech integument I. Electrogenic Na^+ transport and current fluctuation analysis of the apical Na+ channel. *J. Comp. Physiol. B Biochem. Syst. Environ. Physiol.* **163**, 153–159.

Weber, W. M., Blank, U. and Clauss, W. (1995). Regulation of electrogenic Na^+ transport across leech skin. *Am. J. Physiol. Regul. Integr. Comp. Physiol.* **268**, 605–613.

Weihrauch, D. (2006). Active ammonia absorption in the midgut of the tobacco hornworm Manduca sexta L.: transport studies and mRNA expression analysis of a Rhesus-like ammonia transporter. *Insect Biochem. Mol. Biol.* **36**, 808–821.

Weihrauch, D., Becker, W., Postel, U., Riestenpatt, S. and Siebers, D. (1998). Active excretion of ammonia across the gills of the shore crab Carcinus maenas and its relation to osmoregulatory ion uptake. *J. Comp. Physiol. B Biochem. Syst. Environ. Physiol.* **168**, 364–376.

Weihrauch, D., Ziegler, A., Siebers, D. and Towle, D. W. (2002). Active ammonia excretion across the gills of the green shore crab Carcinus maenas : participation of Na^+/K^+-ATPase, V-type H^+-ATPase and functional microtubules. *J. Exp. Biol.* **205**, 2765–2775.

Weihrauch, D., Morris, S. and Towle, D. W. (2004). Ammonia excretion in aquatic and terrestrial crabs. *J. Exp. Biol.* **207**, 4491–4504.

Weihrauch, D., Wilkie, M. P. and Walsh, P. J. (2009). Ammonia and urea transporters in gills of fish and aquatic crustaceans. *J. Exp. Biol.* **212**, 1716–1730.

Weihrauch, D., Donini, A. and O'Donnell, M. J. (2012a). Ammonia transport by terrestrial and aquatic insects. *J. Insect Physiol.* **58**, 473–487.

Weihrauch, D., Chan, A. C., Meyer, H., Döring, C., Sourial, M. and O'Donnell, M. J. (2012b). Ammonia excretion in the freshwater planarian Schmidtea mediterranea. *J. Exp. Biol.* **215**, 3242–3253.

Weiner, I. D. and Verlander, J. W. (2014). Ammonia transport in the kidney by Rhesus glycoproteins. *Am. J. Physiol. Renal Physiol.* **306**, F1107–F1120.

Wenning, A. (1996). Managing high salt loads: from neuron to urine in the leech. *Physiol. Zool.* **69**, 719–745.

Wilkie, M. P. (1997). Mechanisms of ammonia excretion across fish gills. *Comp. Biochem. Physiol. Part A Physiol.* **118A**, 39–50.

Wilson, R. W., Wright, P. M., Munger, S. and Wood, C. M. (1994). Ammonia excretion in freshwater rainbow trout (Oncorhynchus mykiss) and the importance of gill boundary layer acidification : Lack of evidence for Na^+/NH_4^+ exchange. *J. Exp. Biol.* **191**, 37–58.

Wilson, J. M., Randall, D. J., Donowitz, M., Vogl, A. W. and Ip, A. K. (2000). Immunolocalization of ion-transport proteins to branchial epithelium mitrochondria-rich cells in the mudskipper (Periophthalmodon schlosseri). *J. Exp. Biol.* **203**, 2297–2310.

Wilson, J. M., Moreira-Silva, J., Delgado, I. L. S., Ebanks, S. C., Vijayan, M. M., Coimbra, J. and Grosell, M. (2013). Mechanisms of transepithelial ammonia excretion and luminal alkalinization in the gut of an intestinal air-breathing fish, Misgurnus anguilliacaudatus. *J. Exp. Biol.* **216**, 623–32.

Wright, P. A. (1995). Ntrogen excretion : Three end products, many physiological roles. *J. Exp. Biol.* **198**, 273–281.

Wright, P. A. and Wood, C. M. (2009). A new paradigm for ammonia excretion in aquatic animals: role of Rhesus (Rh) glycoproteins. *J. Exp. Biol.* **212**, 2303–2312.

Wu, Y., Zheng, X., Zhang, M., He, A., Li, Z. and Zhan, X. (2010). Cloning and functional expression of Rh50-like glycoprotein, a putative ammonia channel, in Aedes albopictus mosquitoes. *J. Insect Physiol.* **56**, 1599–1610.

Zidi-Yahiaoui, N., Callebaut, I., Genetet, S., Le Van Kim, C., Cartron, J.-P., Colin, Y., Ripoche, P. and Mouro-Chanteloup, I. (2009). Functional analysis of human RhCG: comparison with E. coli ammonium transporter reveals similarities in the pore and differences in the vestibule. *Am. J. Physiol. Cell Physiol.* **297**, C537–C547.

Zimmer, A. M., Nawata, C. M. and Wood, C. M. (2010). Physiological and molecular analysis of the interactive effects of feeding and high environmental ammonia on branchial ammonia excretion and Na^+ uptake in freshwater rainbow trout. *J. Comp. Physiol. B.* **180**, 1191–1204.

Zwingmann, C. and Butterworth, R. (2005). An update on the role of brain glutamine synthesis and its relation to cell-specific energy metabolism in the hyperammonemic brain: further studies using NMR spectroscopy. *Neurochem. Int.* **47**, 19–30.

Appendices:

Table 2: Rh protein genes utilized for generation of maximum likelihood tree in figure 9. Accession numbers given are those for GenBank.

Organism	Rh Gene Cluster	Accession Number
Nitrosomonas europaea	Rhp	AAR24581.1
Nephelopsis obscura	Rhp1	KM923907
Geodia cydonium	Rhp1	CAA73029.1
Caenorhabditis elegans	Rhp1 (Rhr-1)	AAF97864.1
Metacarcinus magister	Rhp1	AEA41159.1
Carcinus maenas	Rhp1	AAK50057.2
Manduca sexta	Rhp1	ABI20766.1
Aedes aegypti	Rhp1 (Rh50-1)	AAX19513.1
Aedes aegypti	Rhp1 (Rh50-2)	AY926464
Drosophila melanogaster	Rhp1	AF193812
Crassostrea gigas	Rhp1	EKC21768.1
Strongylocentrotus purpuratus	Rhp1	XP_789738.3
Helobdella robusta	Rhp1	XP_009016010.1
Takifugu rubripes	Rhag	AAV28817.1
Danio rerio	Rhag	AAQ10011.1
Ambystoma tigrinum	Rhag	AAV28818.1
Xenopus laevis	Rhag	BAB13345.1
Mus musculus	Rhag	AAC25155.1
Bos taurus	Rhag	AAG38955.1
Homo sapiens	RhAG	AAC04247.1
Macaca mulatta	Rhag	AAG00307.1
Oncorhynchus mykiss	Rhag	ABV24962.1
Danio rerio	Rhbg	AAQ09527.1
Takifugu rubripes	Rhbg	AAM48577.1
Tetraodon nigroviridis	Rhbg	AAY41906.1
Xenopus laevis	Rhbg	AAR08675.1
Mus musculus	Rhbg	AAF19371.1
Canis familiaris	Rhbg	AAV40851.1
Homo sapiens	RhBG	AAG01086.1
Oncorhynchus mykiss	Rhbg (Rhbg-1)	ABO16485.1
Sus scrofa	Rhbg	AAK14651.1
Oncorhynchus mykiss	Rhcg	AAU89494.1
Danio rerio	Rhcg	AAM90586.1
Takifugu rubripes	Rhcg (Rhcg2)	AAM48579.1
Oryctolagus cuniculus	Rhcg	AAK14653.1
Xenopus laevis	Rhcg	AAH84943.1
Bos taurus	Rhcg	AAK14650.1
Homo sapiens	RhCG	AAF19372.1
Takifugu rubripes	Rhcg (Rhcg1)	AAM48578.1
Mus musculus	Rhcg	AAF19373.1
Canis_familiaris	Rh30	AAX39718.1
Bos taurus	Rh30	AAD11526.1
Homo sapiens	Rh30	CAA38401.1
Oncorhynchus mykiss	Rh30	AAP87367.1
Mus musculus	Rh30	AAC25123.1
Xenopus laevis	Rh30	AAR00222.1
Danio rerio	Rh30	AAU81655.1
Takifugu rubripes	Rh30	AAM48580.2
Salmo salar	Rh30	AAR01778.1

Figure 15. Experimental timeline for ammonia excretion experiments. **A**, Whole animal pharmacology experiments. **B**, Ussing chamber experiments. **C**, Environmental pH stress experiments. **D**, Feeding experiments. **E**, High environmental ammonia experiments.

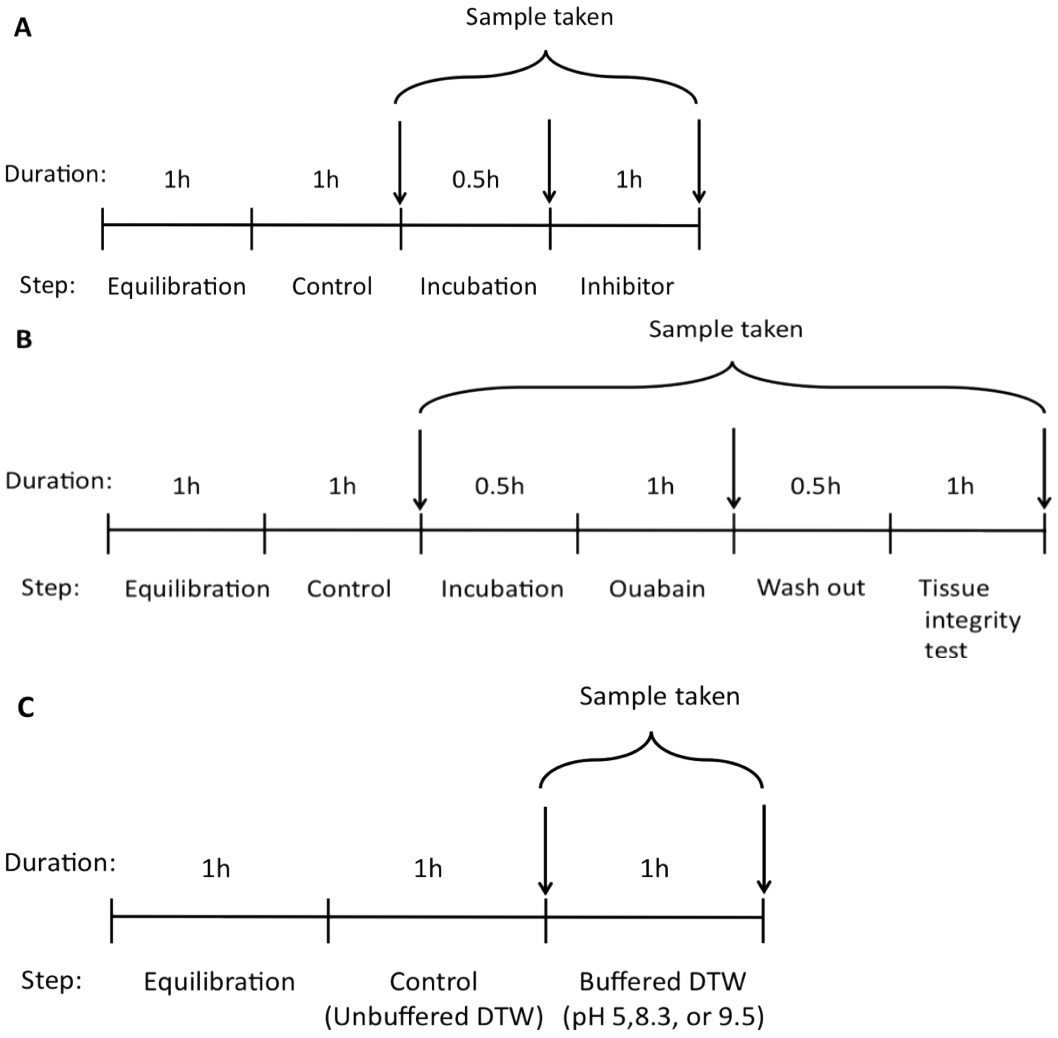

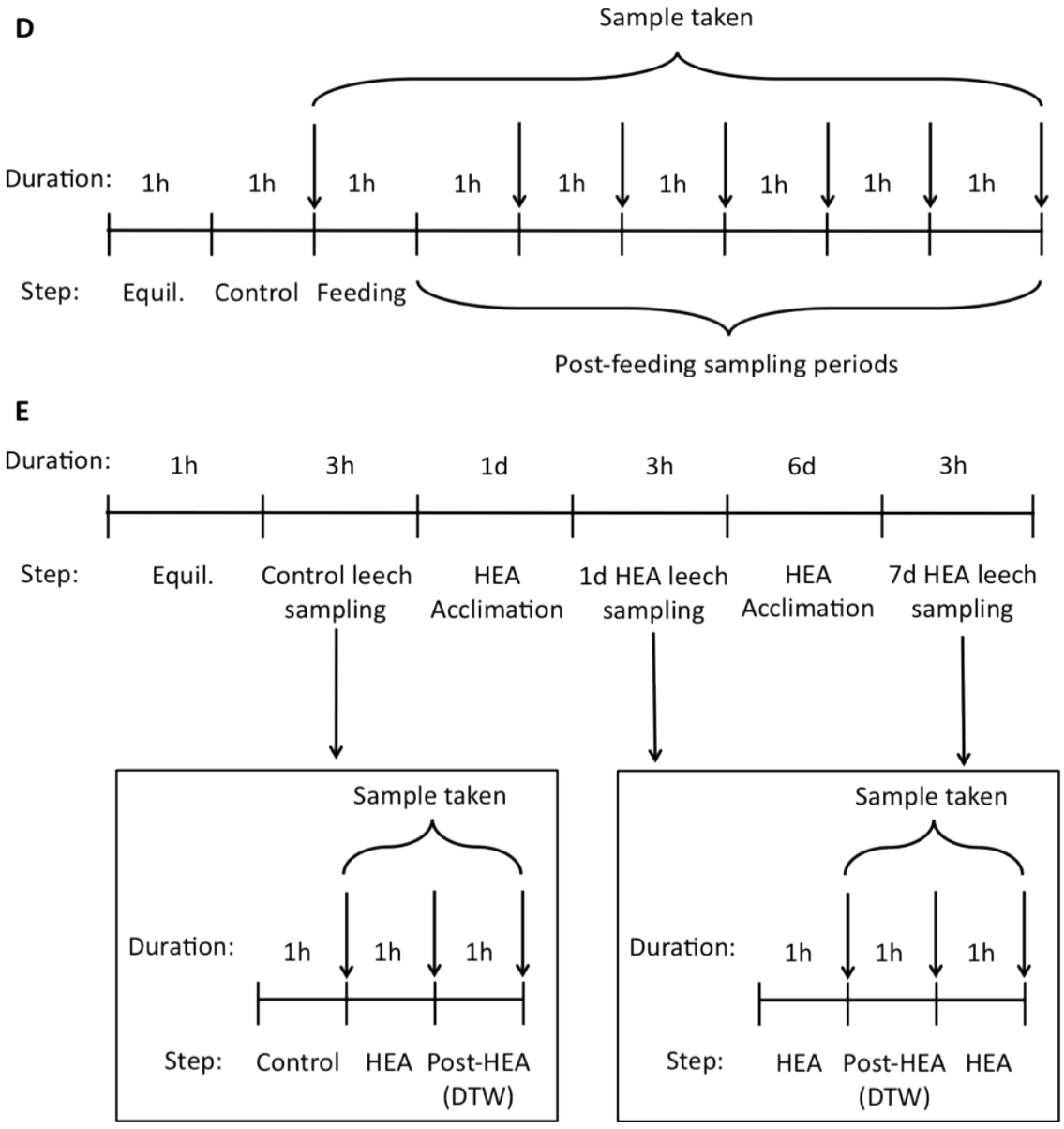
D
Sample taken
Duration:
1h
1h
1h
1h
1h
1h
1h
1h
1h
Step:
Equil.
Control
Feeding
Post-feeding sampling periods
E
Duration:
1h
3h
1d
3h
6d
3h
Step:
Equil.
Control leech sampling
HEA Acclimation
1d HEA leech sampling
HEA Acclimation
7d HEA leech sampling
Sample taken
Duration:
1h
1h
1h
Step:
Control
HEA
Post-HEA (DTW)
Sample taken
Duration:
1h
1h
1h
Step:
HEA
Post-HEA (DTW)
HEA